

**SEDIMENTATION STUDIES FOR PONG
RESERVOIR, HIMACHAL PRADESH**

**NATIONAL INSTITUTE OF HYDROLOGY
JALVIGYAN BHAVAN
ROORKEE - 247667 (UTTARAKHAND)
2015-2016**

Director	Sh. R. D. Singh
Division	Surface Water Hydrology Division
Divisional Head	Dr. Rakesh Kumar, Scientist-G

STUDY TEAM

Principal Investigator	Dr. A. R. Senthil Kumar, Scientist-E, SWHD
Other members of Study Team	i) Dr. Manohar Arora, Sc D, SWHD ii) Dr. Suhas D Khobragade, Sc E, HID iii) Dr. Avinash Agarwal, Sc, G SWHD iv) Dr. Sanjay Jain, Sc G, WRSD v) Sh. Digambar Singh, Sc C, SWHD vi) R. K. Nema, PRA, SWHD

ABSTRACT

Large reservoirs have been constructed to meet the estimated demands for various purposes during the low flow season. The performance of the reservoirs gets reduced mainly due to the high sediment flow resulting from the unpredicted activities in the catchment of the reservoirs. Empirical and physically based models have been applied to estimate the sediment yield expected to be observed at the reservoir site. Recent applications of Artificial Neural Networks (ANN) in modelling the simulation of sediment yield demonstrate its performance over the traditional models. This study presents the method to predict the reservoir capacity using ANN. The sediment yield at Pong reservoir located in Beas has been modelled using ANN by considering the rainfall and discharge as input to the model. The rainfall and discharge for future 25, 50, 75 and 100 years have been generated by the time series modelling. The sediment yield for the same period has been estimated using the best ANN model with the input data as generated series of rainfall and flow volume. The unit weight of deposited sediment in the reservoir has been computed from particle size distribution of suspended sediment concentration and the method of reservoir operation by the procedure suggested by USBR, from the sediment volume observed by hydrographic survey and assuming porosity of uniformly distributed sediment in the reservoir. The consolidated unit weights of the sediment have been computed by the equation proposed by Miller of USBR and frequency analysis of unit weights derived from particle size distribution. The consolidated unit weights computed by different methods have been used to compute the possible range of sediment volume expected to be deposited in the reservoir for the future 25, 50, 75 and 100 years. The computed sediment volume has been distributed in the reservoir by empirical area reduction method.

Chapter 1

Introduction

Many major reservoirs have been commissioned during the last sixty years. Over the years, the performance of the reservoirs gets reduced mainly due to the high sediment flow resulting from the unpredicted activities (land use changes) in the catchment of the reservoirs. Recent survey of Indian reservoirs shows that sediment yield from the catchment has been many fold than the sediment inflow considered during the design of the reservoirs. During the past 50 years, average sediment inflow to the reservoirs has been observed to be about 200 percent more than that assumed during the design (Tejwani, 1984). Some of reservoirs have lost up to 60 percent of their designed capacity, eg., Nizam Sagar reservoir in Andhra Pradesh. Consideration of sediment yield from the catchment area over the life period of the reservoir in view of the high sediment inflow has become important to evolve future operating policy to maximize the benefits from the water releases for various sectors. The upstream activities of the catchment induce higher sediment load in Beas river and it affects the designed life of the reservoir Pong.

In this report, a methodology has been developed to assess the future sediment rates and the life of the Pong reservoir, which will help reservoir authorities in planning for irrigation, water supply, flood control and hydro power generation. An ANN model is developed to simulate the monthly sediment yield at Jwala Mukhi upstream of Pong reservoir using monthly rainfall at Dehra Gopipur, Haripur, Nangal Chowk and Pong Dam, monthly flow volume at Jwala Mukhi and monthly sediment load at Jwala Mukhi. Back propagation feed forward neural network is used for the development of ANN model. The statistical indices such as coefficient of correlation (CORR), Nash-Sutcliffe model efficiency (EFF) and root mean squared error (RMSE) are used to analyze the performance of ANN model. The data of rainfall and flow volume for next 25, 50, 75 and 100 years have been generated by the time series modelling. The sediment yields for the same period have been simulated using the best ANN model with the input data as generated series of rainfall and flow volume. The unit weight of the sediment has been computed from particle size distribution, porosity of uniformly distributed sediment, hydrographic survey and frequency analysis. The consolidated unit weights of the sediment have been computed by the Miller's equation and frequency analysis of unit weights derived from particle size distribution. The consolidated unit weights computed by different methods have been used to compute the possible range of

sediment volume expected to be deposited in the reservoir for the future 25, 50, 75 and 100 years. The computed sediment volume has been distributed in the reservoir by empirical area reduction method.

Chapter 2 Review of Literature

2.1 Estimation of sediment yield

Estimation of sediment load has become important in river engineering practices, river training, river management and the design, maintenance and operation of hydraulic structures mainly power plants. Another important use is in water quality monitoring (Nagy et al., 2002). The estimation of sediment from the catchment has been the subject of research for several decades and has been difficult task due to the complex nature of the sedimentation process. The sedimentation process depends upon the characteristics of basin and river which include climate, land slope and topography, land cover and pattern of land use (Shahin, 1993). Measurement of sediment load in some of the rivers dates back to the last century. Recent publications reveal that sediment load has been observed to understand sediment process in the watershed as well as to predict the sediment load (Nagle et al., 2007; Woodward and Walling, 2007; Kido et al., 2007; Smith, 2008; Horowitz et al., 2008; Mano et al., 2009; Deasy et al., 2009; Dugan et al., 2009).

Several methods have been proposed to predict sediment load based on the properties of flow and sediment. Models such as black box models, regression based models and physically based models have been developed for computing the sediment yield (Garde and Rangaraju, 1985; Graf, 1984; Rijn, 1984 a,b,c; Tayfur, 2002; Gao and Pasternack, 2007; Doomen et al., 2008; Parajuli et al., 2009). During 1945 to 1965, an empirical method for computing the upland soil losses was evolved based on statistical analysis from the experiment conducted from many small plots in the states of USA, which was named as Universal Soil Loss Equation (USLE) (Schwab, et al. 1993). It has been widely used in many countries to estimate the sediment yield from the watersheds despite its simplification of many variables involved. The USLE is given as

$$A = RKLSCP \quad (2.1)$$

where A is average annual soil loss per unit area, R is rainfall and runoff erosivity index for geographic location, K is soil erodibility factor, L is slope length factor, S is slope steepness factor, C is cover management factor and P is conservation practice factor. USLE predicts average annual gross erosion as a function of rainfall energy. To improve the prediction capability of USLE, the rainfall energy factor is replaced with a runoff factor and this is called as modified universal soil loss equation (MUSLE). Sediment yield prediction is improved

because runoff is a function of antecedent moisture condition as well as rainfall energy. MUSLE eliminates the need for delivery ratio and it allows the equation to be applied to individual storm events. The MUSLE is given as

$$Y = 11.8(Qq)^{0.56} KLSCP \quad (2.2)$$

where Y is the single storm sediment yield (*tons*), Q is the runoff (m^3), q is peak storm discharge (m^3/s) and K , L , S , C and P are the standard USLE terms used in equation in (2.1) (Neitsch et al., 2005).

Physically based semi distributed models such as Soil and Water Assessment Tool (SWAT) and Annualized Agricultural Non Point Source (AnnAGNPS) were developed to estimate the sediment load wherein modified USLE was used for the estimation of sediment yield (Parajuli et al., 2009).

Development of many process-based physical models for computing soil erosion and deposition in the basin are reported in the literature. The models developed are 1D, 2D, 3D considering numerical solution of differential conservation equations of mass and momentum of flow along with sediment mass continuity equation. The models applied to different basins are HEC-6, MOBED, IALLUVIAL, FLUVIAL 11, CHARIMA, SEDICOU, OTIS, EFDCID, MIKE3, HEC-RAS, 3ST1D, SERATRA, SUTRENCH-2D, MOBED2, FLUVIAL 12, MIKE 21, DELFT 2D, ECOMSED, CH3D-SED, MIKE 3, DELFT 3D and TELEMAC (Papanicolaou et al., 2008). Water Erosion Prediction Project (WEPP) model is a process-based model based on infiltration theory, hydrology, soil physics, plant science, hydraulics and erosion mechanics (Pandey et al., 2009).

Discrepancies between physically based sediment transport models and measurements are observed due to the oversimplification of the problem by using an inappropriate model, inappropriate input data, lack of appropriate data for model calibration, unfamiliarity with the limitations of the sediment transport equations and computational errors of numerical schemes. The applicability of these models to all rivers is limited due to the simplification of important parameters and boundary conditions considered (Nagy et al., 2002). Moreover, these models warrant huge amount of data and require substantial computational time to implement. Models such as black box models like Autoregressive (AR), Autoregressive Moving Average (ARMA) and Autoregressive Integrated Moving Average (ARIMA); and regression based models like Multiple Linear Regression (MLR) have been applied under limited data availability conditions. But the results obtained from these models are not always satisfactory. In recent years, the newer techniques such as Artificial Neural Networks

(ANN) and Fuzzy logic are being explored and the proven better performance of these techniques over the conventional models has enabled the modelers to apply in many real world problems. The main advantage of the ANN models over traditional models is that they do not require information about the complex nature of the underlying process under consideration to be explicitly described in mathematical form.

ANNs have been found in many real world applications such as image processing, speech processing, control engineering, medicine, classification due to its robustness in noisy environment and flexibility in solving the problems (Jain et al., 2004). Neural networks approach has been applied in many areas of water resources due to its capability in representing any nonlinear processes by given sufficient complexity of the trained networks (ASCE 2000a, 2000b; Govindaraju and Rao, 2000; Maier and Dandy, 2000). Applications of ANNs in water resources include rainfall-runoff modelling (Srinivasulu and Jain, 2009), river flow forecasting (Fernando and Shamseldin 2009), rainfall prediction (Kalteh and Berndtsson, 2007), modelling of evaporation (Keskin and Terzi, 2006), modelling of evapotranspiration (Parasuraman et al., 2006), impact of climate change on streamflow (Chen et al., 2008), Salt water intrusion (Bhattacharjya et al., 2007), ground water pollution (Singh et al., 2004), reservoir operation (Jain et al., 1999), soil water retention (Jain et al., 2004), sediment rating curve (Jain, 2008), suspended sediment concentration (Cobaner et al., 2009) and sediment yield (Raghuwanshi et al., 2006).

2.2 Application of ANN in sediment process

Many applications of ANN in modelling of sediment process are reported in the literature. Some of them are reviewed in detail. Jain (2001) used ANN approach to establish stage-discharge-sediment concentration relationship and compared with conventional sediment rating curves. It was shown that ANN results were very close to the observed values than the conventional technique. Nagy et al. (2002) selected the input neurons based on properties of flow and sediment. The properties considered were tractive shear stress, velocity ratio, suspension parameter, longitudinal slope, water depth ratio, Froude number, Reynolds number, stream width ratio, depth scale ratio and mobility number. The results indicated that ANN models performed better than conventional models of sediment discharge. Cigizoglu (2002) compared the performance of ANN model with empirical sediment rating curves in estimating the suspended sediment concentration and concluded that ANN could model hysteresis in the sediment concentration-water discharge relationship which was impossible with sediment rating curves. Tayfur et al. (2003) developed the ANNs model for

predicting suspended sediment concentration by considering the rainfall intensity and slope as input neurons and compared with the performance of physics-based models. ANN models predicted suspended sediment concentration better than physics-based model. Kisi (2004) predicted the suspended sediment concentration using multi-layer perceptrons (MLP), generalized regression neural networks (GRNN), radial basis function network (RBFN) and multiple-linear regression (MLR) model and the results of all models were compared with each other and it was found that RBFN and GRNN performed better than MLP and MLR in the estimation of sediment load. Kisi (2005) used ANN approach to establish streamflow-suspended sediment relationship and concluded that ANN approach gave better results than regression based sediment rating curve and multiple linear regression models. Cigizoglu and Kisi (2006) found that range dependent neural network (RDNN) was superior to conventional ANN application in estimating suspended sediment concentration. Raghuwanshi et al. (2006) developed ANN models to predict sediment yield on daily and weekly basis for small agricultural watersheds and found that the ANN models performed better than regression models. Lohani et al. (2007) used ANN model for deriving stage-discharge-sediment concentration and compared its results with regression based sediment rating curve. ANN model performed better than regression based sediment rating curve in predicting the suspended sediment concentration. Jain (2008) investigated the ability of compound neural networks (CNN) to model the integrated stage-discharge-suspended sediment relationship. He compared the results of CNN with single ANN and found that CNN results were very close to observed values than single ANN. Cobaner et al. (2009) proposed adaptive neuro-fuzzy approach for estimating the suspended sediment concentration using rainfall, discharge and sediment data of different period. They compared the results of the neuro-fuzzy model with generalized regression neural networks (GRNN), RBNN, MLP and two different sediment rating curves (SRC). It was concluded that neuro-fuzzy approach performed better than other models in estimating the sediment concentration. It was concluded that ANNs model the sediment movement better than the other formulae including regression model. Jothiprakash and Garg (2009) modelled the reservoir sediment volume using ANN with the input as annual rainfall, annual inflow and the capacity of the reservoir and found that ANN performed better than conventional regression analysis.

2.3 Modelling of sediment distribution in reservoir

The distribution of sediment in the reservoir is a complex process and has been modelled by continuity equation and momentum equation of flow and continuity equation of sediment. Studies related to the simulation of delta profile in the reservoirs are reported in the literature but are limited in numbers. Thomas and Prasuhn (1977) studied the sediment deposition in reservoirs by solving the continuity equation of sediment transport for movable bed and the solution was obtained by finite difference scheme. The model results were verified with the laboratory tests. Chen et al. (1978) simulated the reservoir sediment deposition profile by solving numerically the governing equations of sediment laden flow such as continuity and momentum equations and the sediment continuity equation and the simulated profile was compared with measured data from hydraulic model study and it was found that the result was very close to the measured data. Focsa (1980) computed the sediment deposition profile in Iron Gates reservoir in Romania and Yugoslavia by a numerical model after 5 years of dam construction. Miraki (1983) proposed empirical formulae for computing the delta profile based on the analysis of data of some Indian reservoirs. Molanezhad (1984) presented mathematical approach for the reservoir sedimentation and it was evaluated with Gobind sagar reservoir. Okabe et al. (1993) developed a hydraulic simulation model for a one dimensional sedimentation process in a gorge type of reservoirs. Chitale et al. (1998) estimated delta profile in the Indravati reservoir by three methods 1) a mathematical model (MIKE 11) 2) the empirical procedure developed by the U. S. Bureau of Reclamation (USBR) based on the observations about the topset slope, forest slope, and pivot point made when the reservoir in operation 3) a procedure based on sediment distribution following empirical area reduction method. It was reported that the results of all the three methods were comparable.

Successful implementation of numerical models requires large amount of data and proper consideration of boundary conditions. The stability of numerical scheme is of great concern and numerical scheme gives unwanted results in steep slopes which are always present in the bed of reservoirs. To overcome all these difficulties, empirical methods have been proposed by Borland and Miller (1958). The two empirical methods are area increment method and area reduction method. The assumption in area increment method is that the sediment volume above the zero elevation is to be distributed equally at each level of the reservoir. But in the area reduction method the sediment is distributed according to the area design curves for a particular type of reservoir. These methods can be used to revise the elevation-area-capacity curves for a sediment volume as concluded by Chitale et al. (1998).

2.4 Consolidation of sediment in reservoir

The sediment settled in the reservoir is consolidated progressively due to the pressure of stored water and the porosity of the sediment is reduced. Swamee (2001) studied number of soil samples from the reservoirs and proposed equations to get initial (λ_0) and ultimate (λ_∞) porosity of the sediment considering the grain size distribution. He found that the initial and ultimate porosity for uniform sediment were 0.523 and 0.355 respectively. Strand and Pemberton (1987) proposed an equation to compute the consolidated unit weight of sediment for a specified duration from the initial unit weight. Swamee (2001) presented an empirical equation to compute the sediment volume for a particular year by knowing the initial reservoir capacity and expected life of the reservoir.

Chapter 3 Study area

Pong Dam is located on the Beas River, which is one of the five major rivers of the Indus basin. The river Beas flows from the Beas Kund near Rohtang Pass in the upper Himalayas and traverses a total length of about 116 km from the source to the Pong Dam. The reservoir drains a catchment area of 12,562 km² out of which the permanent snow catchment is 780 km². The study area is given as follows:

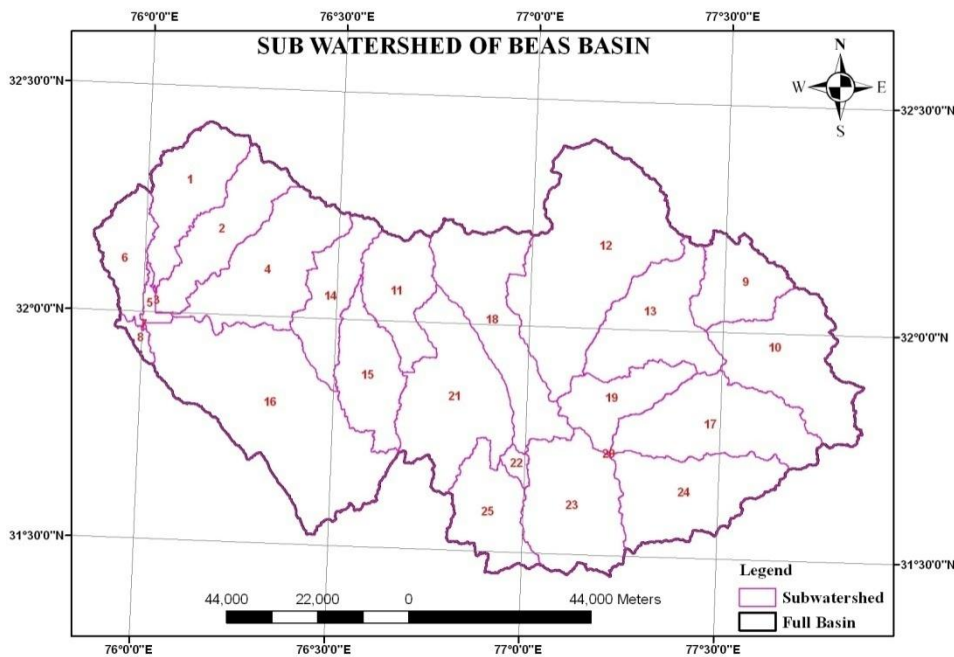


Figure 3.1 Study area of Beas basin upto Pong reservoir

Monsoon rainfall between July and September is a major source of water supply to the reservoir, apart from snow and glacier melt. The dam acts as a sponge for flood flows, and reservoir regulation prevents the inundation of surrounding upland areas from routine flooding during the monsoon season. The reservoir stretch is 42 km long with a maximum width of 19 km, and with a mean depth of 35.7 m. The designed maximum flood discharge of (12,400 m³/s) is discharged through a gated chute spillway located on the left abutment of the dam. The Beas river along with its tributaries generate lot of sediments while flowing through hilly regions and transports the sediment into the Pong reservoir.

3.1 Data used

The monthly rainfall at Dehra Gopipur, Haripur, Nangal Chowk and Pong dam are computed from the daily values of rainfall from 1987 to 2009 (Figures 3.2 to 3.5). The monthly flow volume (Mm^3) (Figure 3.6) and sediment yield ($MTons/month$) at Jwala Mukhi (located on Beas) (Figure 3.7) for the same period are computed from daily values of sediment yield and discharge. The monthly rainfall, flow volume and sediment yield have been used to develop the procedure to predict the elevation-area-capacity curves of Pong reservoir.

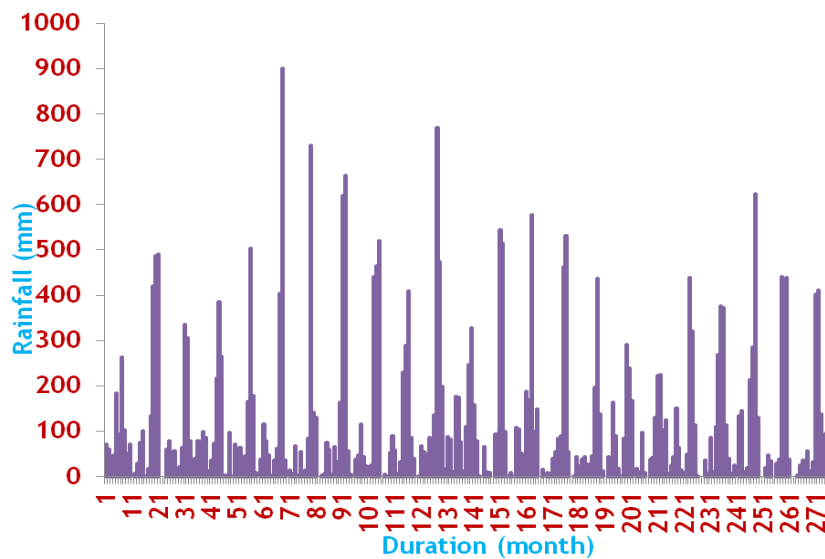


Figure 3.2 Monthly rainfall at Dehra Gopipur

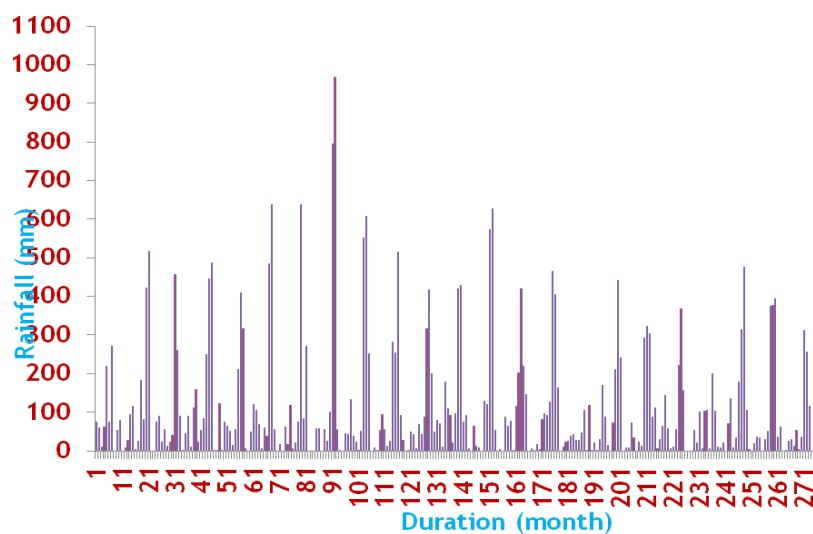


Figure 3.3 Monthly rainfall at Haripur

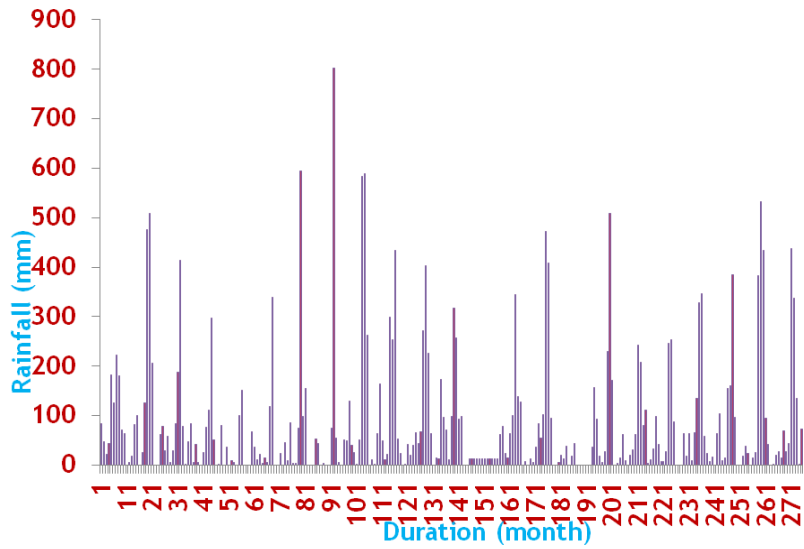


Figure 3.4 Monthly rainfall at Nangal Chowk

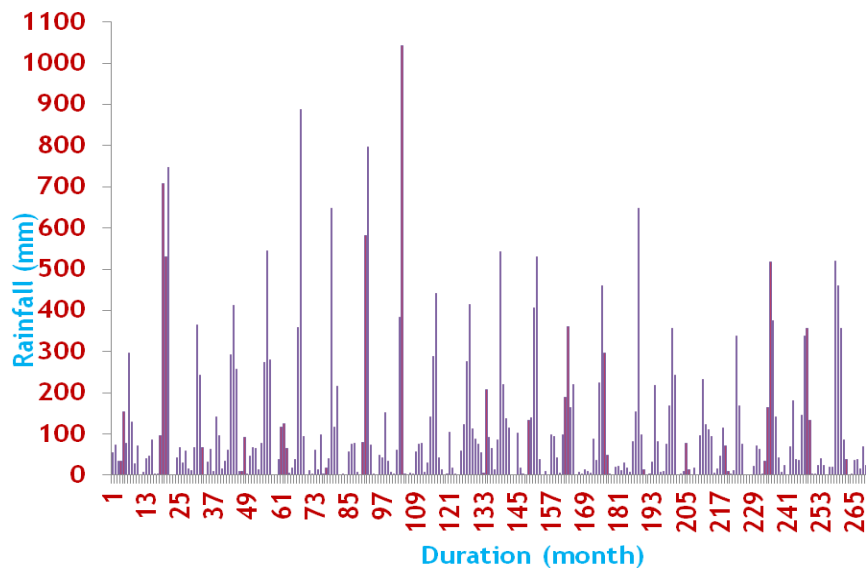


Figure 3.5 Monthly rainfall at Pong Dam

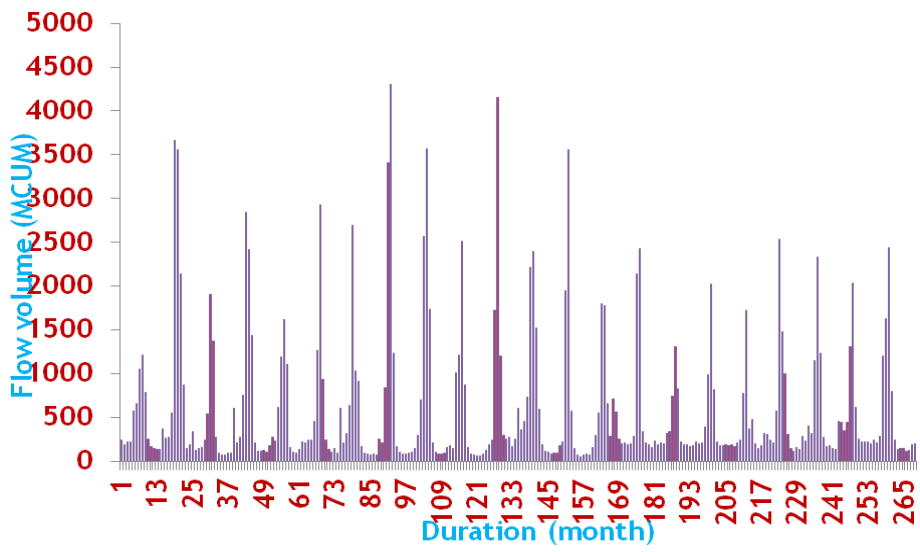


Figure 3.6 Monthly flow volume at Jwala Mukhi

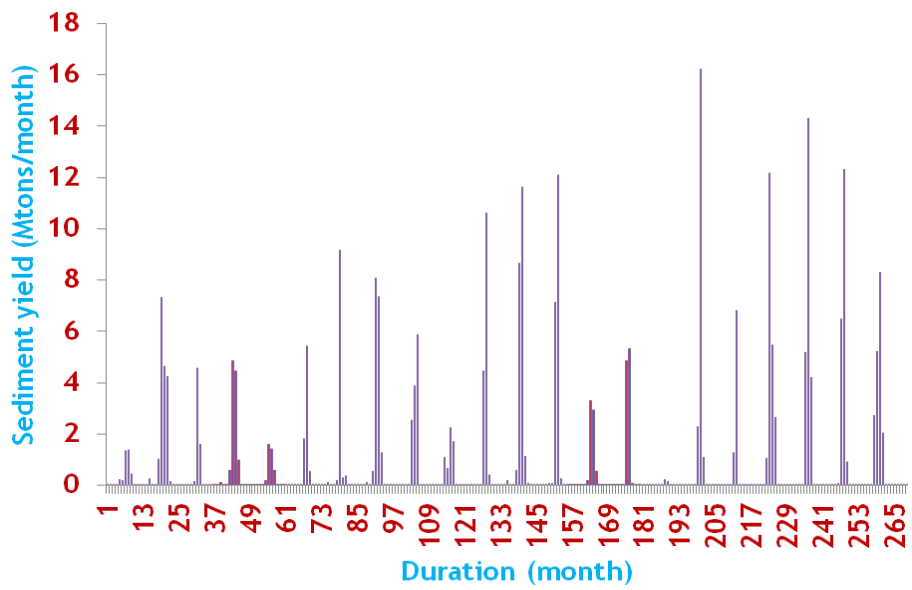


Figure 3.7 Monthly Sediment yield at Jwala Mukhi

Chapter 4 Methodology

The following sections explain the computation of sediment volume and its distribution in the reservoir for future periods considering the consolidation of sediment in the reservoir.

4.1 ANN Model for the Simulation of Sediment Yield

The ANN model is selected for simulating sediment yield due to its successful application and better performance over the conventional models (Jain, 2001; Cigizoglu, 2002; Tayfur et al., 2003; Kisi, 2004; Cigizoglu and Kisi, 2006; Lohani et al., 2007; Cobaner et al., 2009). The correlation analysis of input and output parameter suggests the input vector to the ANN model (Jothiprakash and Garg, 2009). The log sigmoid function is used as output transfer function for modelling the sediment yield process. The number of nodes in the hidden layer plays an important role in simulating the output variable properly (ASCE, 2000a). The number of nodes in the hidden layer is selected by trial and error procedure with reference to the performance indices of ANN model during calibration and validation (Kisi, 2004). The ANN models are trained using back propagation algorithm to get optimal weights for the connections between the nodes. The whole data set are divided into two sets for the training and validation purpose of the ANN model.

4.2 Time Series Modelling

ANN model is very poor in extrapolating the data for unseen range of input vector (Imrie et al. 2000). This property of ANN clearly indicates that it can not be used for the generation of data. Time series models such as AR, ARMA and ARIMA can be used for the generation of data with the sufficient length of available data (Salas et al. 1980). The main components of time series of any hydrological event are trend and other deterministic changes, cycles or periodic changes and components representing stochastic or random variables. The stochastic component is further classified as dependent stochastic component and independent stochastic component. The independent stochastic component is highly random and it follows normal distribution in general. The presence of trend is found out by Kendall's rank correlation test, Mann Kendall test, Spearman's Rho test and linear regression tests (Goel, 2003). Once the presence of trend is detected through above tests, trend can be described by fitting a polynomial to the original time series. The trend is removed from the time series by deducting the polynomial equation. The periodicity present in the time series is

modelled by harmonic analysis and the significant harmonics can be obtained by P_{max} and P_{min} test. After the harmonic analysis, the periodic component can be removed by the smoothed mean and standard deviation of the significant season and the remaining series is called the stochastic component having zero mean and unit variance. The dependent stochastic component is modelled by autoregressive models and the independent component by probability distribution. A general AR model of the order m ($AR(m)$) can be written as follows:

$$z_t = a_1 z_{t-1} + a_2 z_{t-2} + \dots + a_m z_{t-m} + \varepsilon_t \quad (4.1)$$

where z_t is dependent series and ε_t is independent series which can be modelled by probability distribution. ε_t is normally distributed with mean zero and variance σ_ε^2 and is equal to $\sigma_\varepsilon^2 \xi_t$ where ξ_t is standardized normal variable. ξ_t can be represented by normally distributed random numbers. The autoregressive coefficients are estimated by solving the m system of linear equations of autocorrelation function (Salas et al, 1980).

The uniformly distributed random number is generated by mixed congruent or modular method and the normally distributed random number is obtained by transforming uniformly distributed random numbers by Box and Muller method or method based on central limit theorem. The normally distributed random numbers can be generated for any length and it is added with dependent stochastic, cyclic and trend components to get the generated series of hydrological event considered for any length of duration. The rainfall and flow volume are generated using AR models and the best ANN model is used to generate sediment yield for the required period.

4.3 Unit Weight of Deposited Sediment in Reservoir

The computation of unit weight of deposited sediment in reservoir is essential to arrive at the consolidated volume of sediment for required periods using the generated series of sediment yield. The best method of estimation of unit-weight of sediment is from the observation of sediment load at upstream of the reservoir and the volume of sediment in the reservoir by hydrographic survey. But the operation condition of the reservoir sometimes prevents to carry out the hydrographic survey to compute the most accurate value of the unit-weight of the deposited sediment. In such case, the equation proposed by Lara and Pemberton (Strand and Pemberton 1987) can be used to estimate the unit-weight of the

sediment from the proportion of particle size distribution of suspended sediment concentration and the method of reservoir operation and it is given as:

$$W = W_c P_c + W_m P_m + W_s P_s \quad (4.2)$$

where W is unit weight in kg/m^3 , P_c , P_m , P_s are percentages of clay, silt and sand of the incoming sediment respectively and W_c , W_m , W_s are initial unit weights of clay, silt and sand respectively. The classification of sediment according to size as proposed by the American Geophysical Union can be used to estimate the percentages of clay, silt and sand and is given in Table 4.1. The values of W_c , W_m and W_s are obtained from the Table 4.2.

Table 4.1 Soil classification by American Geophysical union

Sediment type	Size range (mm)
Clay	Less than 0.004
Silt	0.004 to 0.0625
Sand	0.0625 to 2.0

Table 4.2 Coefficient values for Lara-Pemberton equation

Operational Condition of the reservoir	Initial weight, kg/m^3		
	W_c	W_m	W_s
Continuously submerged	416	1121	1553
Periodic drawdown	561	1137	1553
Normally empty reservoir	641	1154	1553
Riverbed sediment	961	1170	1553

4.4 Estimation of Consolidated Unit Weight of Sediment

4.4.1 Consolidated Unit Weight of Sediment by Empirical Method

The average unit weight of all sediment deposited during t years of consolidation is computed using the equation presented by Miller (1953) and is given as

$$W_t = W_1 + 0.4343B \left[\frac{t}{t-1} (\ln t) - 1 \right] \quad (4.3)$$

where W_t is the average unit weight after t years of consolidation, W_1 is the initial unit weight and B is a constant and is given as

$$B = B_c P_c + B_m P_m + B_s P_s \quad (4.4)$$

where P_c, P_m, P_s are percentages of clay, silt and sand of the incoming sediment respectively and B_c, B_m, B_s are unit weights of clay, silt and sand respectively. The values of B_c, B_m and B_s are obtained from Table 4.3.

Table 4.3 Coefficient values for the calculation of consolidated unit weights

Operational Condition	B, kg/m^3		
	Sand	Silt	Clay
Continuously submerged	0	91	256
Periodic drawdown	0	43	171
Considerable drawdown	0	16	96
Normally empty reservoir	0	0	0

4.4.2 Consolidated Unit Weight of Sediment by Porosity of the Sediment

Swamee (2001) have analyzed number of soil samples of the reservoirs and have found the value of initial (λ_i) and ultimate (λ_∞) porosity of uniformly distributed sediment as 0.523 and 0.355 respectively. The following equation can be used to find the initial and ultimate unit weight of the sediment by assuming initial and ultimate porosity as 0.523 and 0.355.

$$\lambda = 1 - \frac{\rho_{bulk}}{\rho_{particle}} \quad (4.5)$$

where ρ_{bulk} is unit weight of the sediment and $\rho_{particle}$ is particle density which is 2650 kg/m^3 . If the time for which the reservoir gets silted up is known, the unit weight of the sediment can be interpolated linearly for any particular year.

4.4.3 Consolidated Unit Weight of Sediment by Frequency Analysis

Frequency analysis helps to identify the statistical population of random variable from which the sample measurements have come from (Ojha et al. 2008). Probability statements about the future occurrences of random variable can be made once the population distribution is identified. The possible distribution to represent any hydrological random variable includes Generalized logistic (GLO), Generalized extreme value (GEV), Generalized normal, Pearson type III and generalized Pareto, all are three parameter distributions. The parent distribution, four parameter Kappa distribution, is considered to simulate large sample from the measurement values and from which the suitable population distribution can be identified

from goodness of fit measures of each possible distribution considered. The probability density function $f(x)$, cumulative distribution function $F(x)$ and quintile function $x(F)$ of Kappa distribution is given as follows (Hosking and Wallis 1997):

$$f(x) = \alpha^{-1} \left\{ 1 - \frac{k(x-\xi)}{\alpha} \right\}^{\frac{1}{k-1}} \{F(x)\}^{1-h} \quad (4.6)$$

$$F(x) = \left[1 - h \left\{ 1 - \frac{k(x-\xi)}{\alpha} \right\}^{\frac{1}{k}} \right]^{\frac{1}{h}} \quad (4.7)$$

$$x(F) = \xi + \frac{\alpha}{k} \left\{ 1 - \left(\frac{1-F^h}{h} \right)^k \right\} \quad (4.8)$$

where ξ (location), α (scale), k , h are parameters and F is the probability of non exceedance.

The parameters of any distribution can be estimated by Graphical method, Method of Moments (*MOM*), Probability Weighted Moments (*PWM*) and L-moments. If *PDF* be denoted by $F = F(x) = P[X \leq x]$, then *PWMs* are the moment of the function $x(F)$, and they are expressed as

$$M_{i,j,k} \equiv E \left[x^i F^j (1-F)^k \right] = \int_0^1 \left[x(F)^i F^j (1-F)^k \right] dF \quad (4.9)$$

where $M_{i,j,k}$ is the *PWM* of the order of i, j and k ; and E is the expectation operator.

L-moments are linear combination of order statistics which are robust to outliers and are unbiased for small samples. L-moments are identified as linear combination of probability weighted moment (*PWM*) and first four L-moments are given as

$$\lambda_1 = \beta_0 \quad (4.10a)$$

$$\lambda_2 = 2\beta_1 - \beta_0 \quad (4.10b)$$

$$\lambda_3 = 6\beta_2 - 6\beta_1 + \beta_0 \quad (4.10c)$$

$$\lambda_4 = 20\beta_3 - 30\beta_2 + 12\beta_1 + \beta_0 \quad (4.10d)$$

L-moments produce quintile estimates with lower root mean squared error than unbiased alternatives. The unbiased estimates of *PWMs* for any distribution can be computed as follows:

$$b_0 = \frac{1}{n} \sum_{j=1}^n x_j \quad (4.11a)$$

$$b_1 = \sum_{j=1}^{n-1} \left[\frac{(n-j)}{(n)(n-1)} \right] x_j \quad (4.11b)$$

$$b_2 = \sum_{j=1}^{n-2} \left[\frac{(n-j)(n-j-1)}{(n)(n-1)(n-2)} \right] x_j \quad (4.11c)$$

$$b_3 = \sum_{j=1}^{n-3} \left[\frac{(n-j)(n-j-1)(n-j-2)}{(n)(n-1)(n-2)(n-3)} \right] x_j \quad (4.11d)$$

where x_j represents the order values of random variable with x_1 as the largest value and x_n as the smallest value. The L-moment ratios which are used for expressing the parameter estimates are expressed as L-coefficient of variation (τ_1) = λ_1 ; L-skewness (τ_3) = $\frac{\lambda_3}{\lambda_2}$ and L-

kurtosis (τ_4) = $\frac{\lambda_4}{\lambda_3}$. The sample estimates of L-moments are calculated by replacing

b_0, b_1, b_2 and b_3 for $\beta_0, \beta_1, \beta_2$ and β_3 in equations 4.10a to 4.10d. The goodness-of-fit measure for each distribution is given as

$$Z^{DIST} = (\tau_4^{DIST} - \tau_4^R + B_4) / \sigma_4 \quad (4.12)$$

where *DIST* can be any of the three parameter distributions such as generalized logistic (GLO), Generalized extreme value (GEV), Generalized normal, Pearson type III and generalized Pareto; τ_4^{DIST} is L-kurtosis of the fitted distribution; τ_4^R is regional average of L-kurtosis; B_4 is the bias of τ_4^R . The standard deviation of τ_4^R is given as

$$\sigma_4 = \left[(N_{sim} - 1)^{-1} \left\{ \sum_{m=1}^{N_{sim}} (\tau_4^{[m]} - \tau_4^R)^2 - N_{sim} B_4^2 \right\} \right]^{\frac{1}{2}} \quad (4.13)$$

The bias of τ_4^R is given as

$$B_4 = N_{sim}^{-1} \sum_{m=1}^{N_{sim}} (\tau_4^{[m]} - \tau_4^R) \quad (4.14)$$

where $\tau_4^{[m]}$ is L-kurtosis for N_{sim} of realizations of a region with N sites by fitting kappa distribution to the regional average L-moment ratios, τ^R (L-Coefficient of Variation), τ_3^R (L-Skewness), and τ_4^R (L-kurtosis). If $|Z^{DIST}| \leq \pm 1.64$, the fitness of the considered distribution is adequate. If any of the considered distribution is not satisfying the goodness-of-fit, Wakebey distribution is selected as best distribution for the measured data. The quantile estimate of Wakebey distribution is given as

$$x(F) = \xi + \frac{\alpha}{\beta} \left\{ 1 - (1-F)^\beta \right\} - \frac{\gamma}{\delta} \left\{ 1 - (1-F)^{-\delta} \right\} \quad (4.15)$$

where ξ (location), α , β , γ , δ are parameters of the distribution. Once the parameters of the distribution are estimated the quantile estimate of any return period can be obtained from the equation of $x(F)$. This method is valid up to the maximum possible consolidation of the sediment in the reservoir.

4.5 Trap efficiency of the reservoir

Swamee (2001) proposed the following equation for the estimation of the trap efficiency of the reservoir

$$\eta = \left[\left(\frac{t}{t_*} \right)^{\frac{1}{q}} + 1 \right]^{-(q+1)} \quad (4.16)$$

where t is the year for which the trap efficiency is to be computed; t_* is the time for which the reservoir gets silted up; q is transition exponent and can be obtained from the following equation

$$q = 1.4427 \ln \left(\frac{V_i}{v_*} \right) \quad (4.17)$$

where V_i is the initial storage capacity of the reservoir and v_* is the storage capacity at t_* which is obtained from the plot of cumulative volume of deposition V_s vs time.

4.6 Sediment volume prediction

The simulated sediment yield at the reservoir is converted into sediment volume by the assumed unit weight of the sediment. The simulated sediment volume is compared with the volume computed by the empirical formulae given by Swamee (2001) and are given as follows:

$$v = V_i \left[\left(\frac{t^*}{t} \right)^{\frac{1}{q}} + 1 \right]^{-q} \quad (4.18)$$

$$V = V_i - v \quad (4.19)$$

where v is the reservoir capacity for any year t . The sediment volume is computed from equation (4.19). The sediment volume computed by the ANN model and empirical formula are compared with sediment volume measured by hydrographic survey. The consolidated unit weights of sediment after 25, 50, 75, 100 years computed by all three methods mentioned in the above sections, trap efficiency of the reservoir and sediment yield simulated at the reservoir for future 25, 50, 75, 100 years are used to find out possible range of sediment volumes for future 25, 50, 75 and 100 years.

4.7 Sediment Distribution in the reservoir

Borland and Miller (1958) have suggested two methods for the prediction of sediment distribution pattern in the reservoir. The first is called as area increment method and the second is empirical area reduction method.

The basic equation for area increment method (Murthy 1977) is

$$V_s = A_0(H - h_0) + V_0 \quad (4.20)$$

where V_s is the sediment volume to be distributed in the reservoir; A_0 is area correction factor which is the original reservoir area at the new zero elevation at the dam; V_0 is the sediment volume below new zero elevation; H is reservoir depth at the dam i.e., stream bed to maximum normal water surface; h_0 is the depth to which reservoir is completely filled with

sediment i.e., new zero elevation. This method is based on the assumption that the sediment deposition in a reservoir can be approximated by reducing the reservoir area at different elevations by a fixed amount. A series of approximations are involved in this method. The reservoir capacities are calculated based on the reduced areas applying either prismoidal formula or end area method, such that the capacity below maximum normal level is the same as predetermined capacity obtained by subtracting the sediment accumulation with time from the original capacity. The equation mathematically states that the total volume of sediment V_s , consists of that part which is uniformly distributed vertically over the height $(H - h_0)$ plus the portion below the new zero elevation of the reservoir.

The basic equation used to develop the empirical area reduction procedure is

$$S = \int_{ol}^{y_0} A dy + \int_{y_0}^H K a dy \quad (4.21)$$

where S is the total sediment to be deposited in the reservoir; ol is the original zero elevation at the dam; y_0 is the zero elevation at the dam after the sediment inflow period; A =reservoir surface area; dy is the incremental depth; H is the total depth of the reservoir at normal water surface; K is the constant of proportionality for converting relative sediment areas to actual area for a given reservoir and a is the relative sediment area. By integrating and simplifying the equation (4.21), the following relationship can be developed:

$$\frac{1 - v_0}{a_0} = \frac{S - V_0}{H A_0} \quad (4.22)$$

where v_0 is the relative reservoir volume at zero depth; a_0 is the relative reservoir area at new zero elevation; V_0 is total reservoir volume at new zero depth; H is the original depth of the reservoir and A_0 is the total reservoir area at zero depth. By defining two new terms:

$$h(p) = \frac{1 - v(p)}{a(p)} \quad (4.23)$$

$$h'(p) = \frac{S - V(pH)}{H * A(pH)} \quad (4.24)$$

where h is a function of one of four types of theoretical design curves and h' is a function of a particular reservoir and its anticipated sediment storage. The type of the reservoir is determined from $m=x/y$ of log-log plot of depth Vs capacity and it is given as follows:

Table 4.4 Type of the reservoir

m (inverse of slope)	Reservoir type
3.5 to 4.5	Type I (lake)
2.5 to 3.5	Type II (Flood plain foot hill)
1.5 to 2.5	Type III (Hill)
1.0 to 1.5	Type IV (Gorge)

Once the reservoir type is determined, the depth to determine function $h'(p)$ values are determined from equation (4.24) for a sediment volume to be distributed in the reservoir and are plotted Vs relative depth (p) on semi-log paper. The zero depth of the reservoir for a sediment volume is fixed where the depth to determine function curve intercepts the design curves of the type of the reservoir. The relative area A_p is determined from the area design curves and are given as follows:

Table 4.5 Area design curves

Reservoir type	Area design curve (a)
Type I	$5.047 p^{1.85} (1-p)^{0.36}$
Type II	$2.487 p^{0.57} (1-p)^{0.41}$
Type III	$16.967 p^{1.15} (1-p)^{2.32}$
Type IV	$1.486 p^{-0.25} (1-p)^{1.34}$

where p is the relative depth. The sediment area is computed by multiplying the relative area at relative depth with K which is determined from dividing the original area by the relative at zero elevation. The sediment volume is computed by end area method using the computed sediment area at each depth. If the accumulated sediment volume is not equal to sediment volume to be distributed in the reservoir, a new K is computed by multiplying it with the ratio of sediment volume to be distributed to the accumulated sediment volume

and the computation is repeated till the difference between the sediment volume to be distributed and the accumulated sediment volume is zero. The finally adjusted reservoir area and sediment volume is deducted from the original reservoir area and reservoir volume at each depth to get the revised elevation-area-capacity table. The type of the reservoir is to be determined again with revised elevation-area-capacity table. The zero elevation of the reservoir is computed from area increment method if the type of the reservoir is changed and the depth to determine function does not intercept the design curves of the revised type of the reservoir. The sediment volume predicted for future 25, 50, 75 and 100 years are used to predict the elevation-area-capacity table by empirical area reduction method as mentioned above.

Chapter 5

Prediction of elevation-area-capacity curves for pong reservoir

5.1 Development of ANN Model for Sediment Yield

The correlation analysis between monthly rainfall (*mm*) and flow volume (Mm^3) with monthly sediment load (*MTons/month*) is carried out and is given in the following table.

Table 5.1 Correlation analysis of rainfall and flow volume with sediment yield

Parameter	Sediment load at Jwala Mukhi
Rainfall at Dehra Gopipur	0.74
Rainfall at Haripur	0.71
Rainfall at Nangal Chowk	0.68
Rainfall at Pong Dam	0.67
Flow volume at Jwala Mukhi	0.82

The above table indicates that the rainfall at Dehra Gopipur, Haripur, Nangal Chowk and Pong dam and flow volume at Jwala Mukhi have reasonably good correlation with sediment load at Jwala Mukhi. So the following combination is considered as best input vector to the ANN model.

$$Sedyld(t) = f(\text{flowvol}(t), \text{raindehra}(t), \text{rainhari}(t), \text{rainnangch}(t), \text{rainpondam}(t)) \quad (5.1)$$

in which *Sedyld*, *flowvol*, *raindehra*, *rainhari*, *rainnangch* and *rainpondam* are sediment yield, flow volume at Jwala Mukhi and rainfall values at Dehra Gopipur, Haripur, Nangal Chowk and Pong dam respectively. The feed forward ANN is trained with input vector as mentioned above. The monthly data from 1987 to 2007 are considered for the training of the model since it contains the extreme values of sediment load. The data from 2008 to 2009 are considered for the validation of the model. The performance of the ANN model during calibration and validation is given in the following table.

Table 5.2 Results of ANN model during calibration and validation

Model No	Input combinations	ANN Structure	Calibration			Validation		
			CORR	RMSE MTons	EFF%	CORR	RMSE MTons	EFF%
ANNSY1	flowvol(t), raindehra(t), rainhari(t), rainnangch(t), rainpondam(t)	5-1-1	0.86	1.34	75.00	0.94	0.78	88.00
ANNSY2	,,	5-2-1	0.93	0.97	86.60	0.91	1.21	72.00
ANNSY3	,,	5-3-1	0.92	1.66	86.00	0.88	1.65	47.00
ANNSY4	,,	5-4-1	0.96	0.67	93.00	0.80	1.73	42.00

The results from the above table indicate that the performance of the different ANN structure in simulating the sediment yield during calibration is increased as the number of nodes in the hidden layer increased. But it is decreased during the validation of the model. Based on the overall performance of all the combinations, the model ANNSY2 (calibration: CORR= 0.93, RMSE=0.97, EFF=86%; validation: CORR= 0.91, RMSE=1.21, EFF=72%) is selected as the best ANN model for simulating the sediment yield at Jwala Mukhi and the optimum structure of the ANN model is found to be 2 neurons in the hidden layer. The performances of the best ANN model during calibration and validation are given in the following figures.

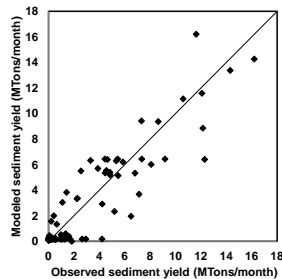


Figure 5.1 The performance of ANN model during calibration at Jwala Mukhi

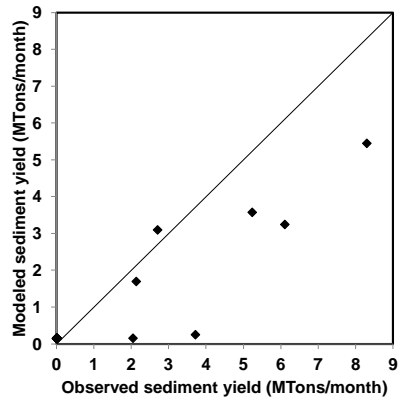


Figure 5.2 The performance of ANN model during validation at Jwala Mukhi

5.2 Simulation of Sediment Yield

The rainfall values at Dehra Gopipur, Haripur, Nangal Chowk and Pong dam and the flow volume at Jwala Mukhi are generated for future 25, 50, 75 and 100 years using the data from 1987 to 2009. The data are generated by AR model of order 1. The properties (mean and standard deviation) of data generated data follow the properties of observed data. The generated data of rainfall and flow volume are used to simulate the sediment yield for future 25, 50, 75 and 100 years using the best ANN model and are presented in Figures 5.3, 5.4, 5.5 and 5.6 respectively. The values of sediment yield at Jwala Mukhi is added with 15 percent for bed load and an average of 30.34 percent (average of sediment yield at the tributaries to main river from 1987 to 2009) for the sediment yield from the small tributaries joining to the reservoir to get the sediment yield at Pong reservoir.

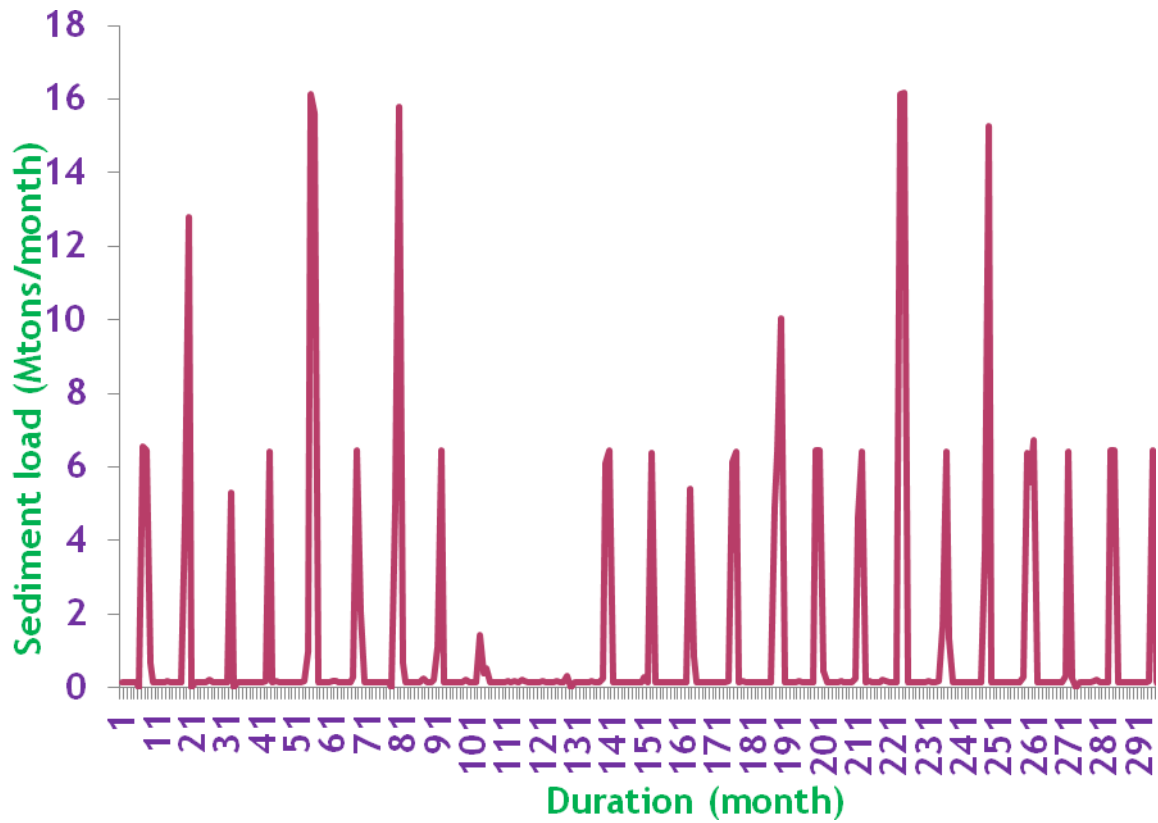


Figure 5.3 The simulated sediment yield for 25 years

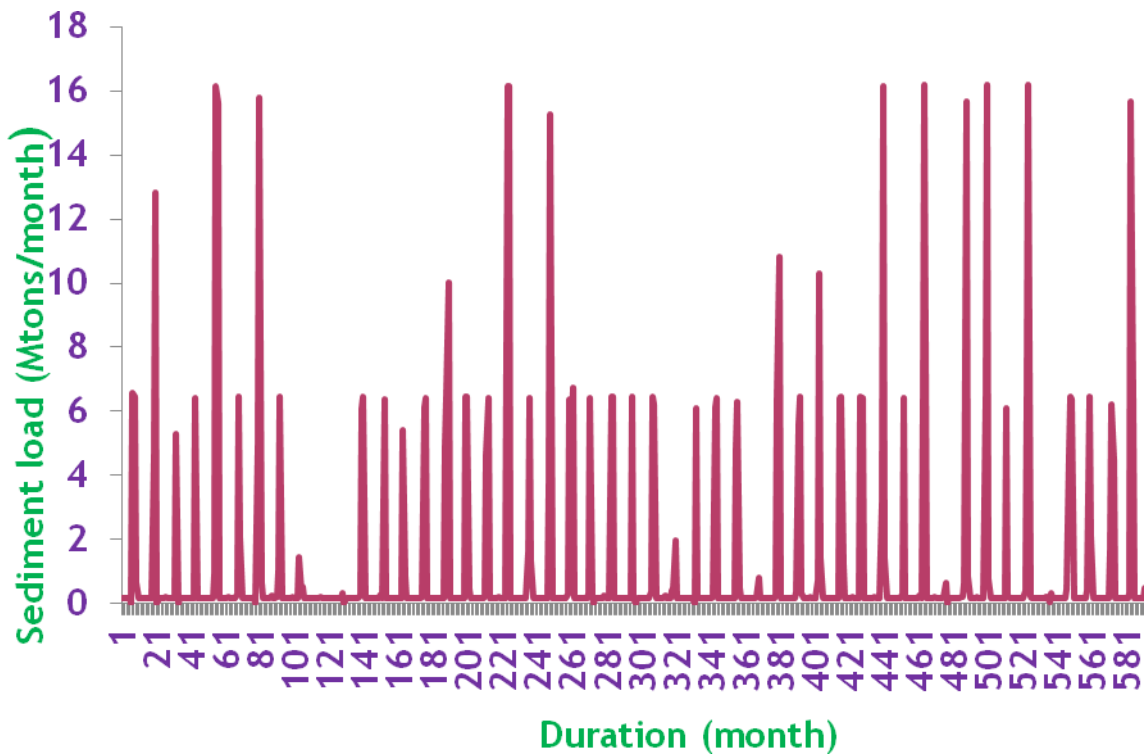


Figure 5.4 The simulated sediment yield for 50 years

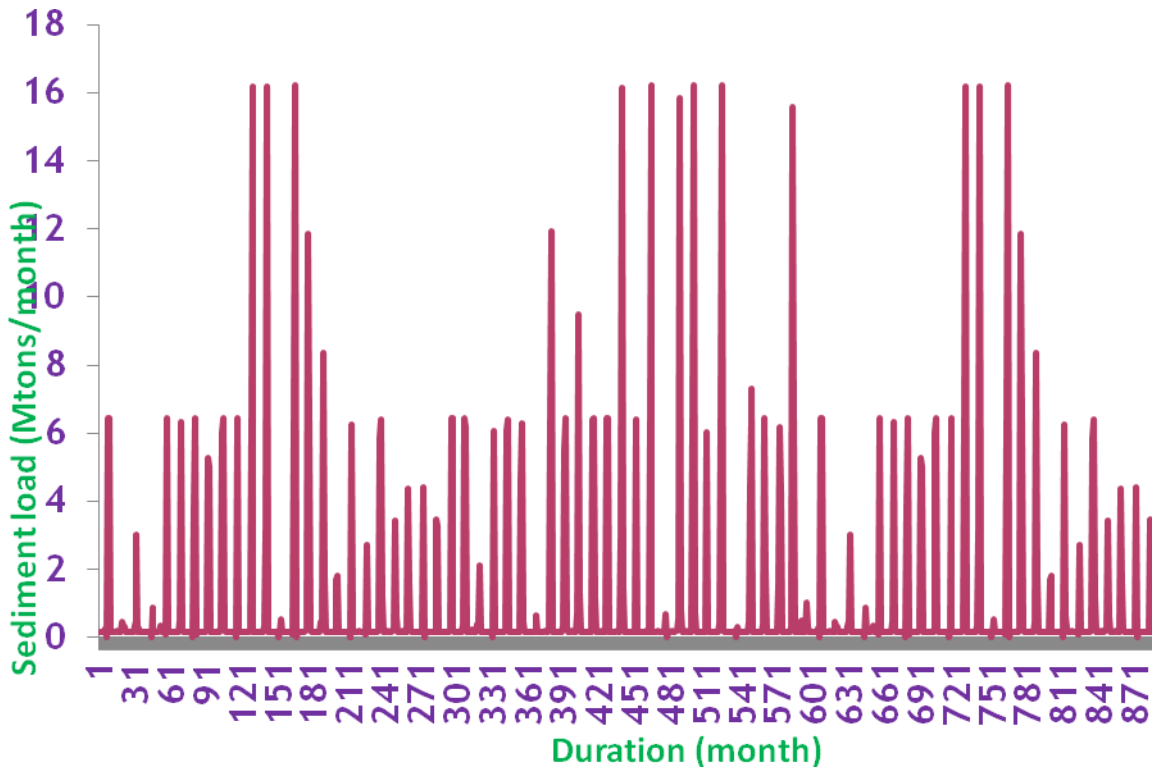


Figure 5.5 The simulated sediment yield for 75 years

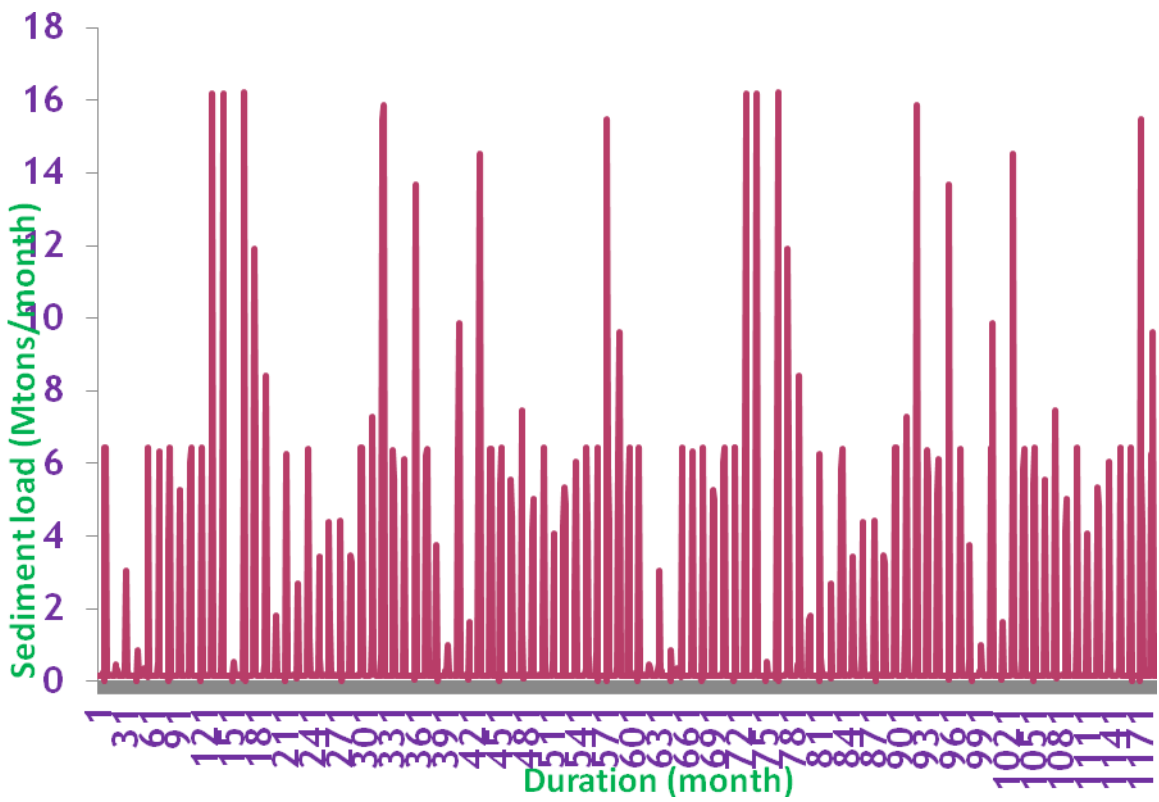


Figure 5.6 The simulated sediment yield for 100 years

5.3 Computation of Unit Weight of Sediment

The suspended sediment concentration observed at Jwala Mukhi is a mixture of coarse sediment (above 0.2 mm), medium sediment (0.075 to 0.2 mm) and fine sediment (below 0.075 mm). According to the soil classification by American Geophysical Union, the observation of sediment at Jwala Mukhi has only silt and sand. The method suggested by Lara and Pemberton (1987) of USBR is used to compute unit weight of sediment by considering the percentages of silt and sand for daily data from 1987 to 2009 and the average unit weight for each year is given in Table 5.3. The average unit weight of sediment for the period from 1987 to 2009 is 1163.633kg/m^3 .

Table 5.3 Average unit weight of sediment from particle size distribution

Year	Percentage		Unit weight kg/m ³
	Silt	Sand	
1987	90.52	9.48	1177.302
1988	89.26	10.74	1182.576
1989	86.03	13.97	1196.017
1990	86.25	13.75	1195.093
1991	87.43	12.57	1190.210
1992	87.86	12.14	1188.410
1993	93.40	6.60	1165.297
1994	87.71	12.29	1189.009
1995	94.86	5.14	1159.231
1996	97.25	2.75	1149.275
1997	95.83	4.17	1155.203
1998	95.66	4.34	1155.910
1999	95.57	4.43	1156.286
2000	95.98	4.02	1154.572
2001	94.78	1.82	1159.542
2002	98.18	1.82	1145.382
2003	97.13	2.87	1149.796
2004	97.18	2.82	1149.578
2005	97.23	2.77	1149.374
2006	97.28	2.72	1149.152
2007	97.33	2.67	1148.907
2008	97.40	2.60	1148.643
2009	97.37	2.63	1148.795

The unit weight of the sediment is calculated from silt retained and silt volume settled by hydrographic survey from 1987 to 2008 and is presented in Table 5.4. The silt retained is obtained by deducting the measured sediment load at downstream of the reservoir from the measured sediment load at upstream of the reservoir. The average unit weight of the sediment from the observed data for the period from 1987 to 2008 is 1129.099 kg/m^3 .

Table 5.4. Unit weight of sediment from hydrographic survey

Year	Silt retained <i>kg</i>	Silt volume settled m^3	Unit weight kg/m^3
1987-88	5950000000	22580000	263.508
1988-89	26215000000	25560000	1025.626
1989-90	10278800000	17740000	579.414
1990-91	18565400000	17930000	1035.438
1991-92	6756400000	10980000	615.337
1992-93	15843800000	8610000	1840.163
1993-94	10525200000	8040000	1309.104
1994-95	29181600000	21160000	1379.093
1995-96	24889200000	21160000	1176.238
1996-97	17669400000	18920000	933.901
1997-98	28929600000	21690000	1333.776
1998-99	29065400000	24370000	1192.671
1999-00	28659400000	22020000	1301.517
2000-01	11134200000	8620000	1291.671
2001-02	19437600000	15820000	1228.673
2002-03	24411800000	20690000	1179.884
2003-04	26916400000	21910000	1228.498
2004-05	19700800000	16330000	1206.418
2005-06	29537200000	23410000	1261.734
2006-07	29332800000	24590000	1192.875
2007-08	24976000000	22030000	1133.727

5.4 Computation of consolidated unit weight of sediment

The consolidated unit weights of sediment for the unit weights obtained from particle size distribution and hydrographic survey of the sediment for future 25, 50, 75 and 100 years are computed using the equation (4.3) given by Miller (1953) and are presented in Table 5.5. The consolidated unit weights of the sediment for the life period of the reservoir are computed by the equation (4.5) assuming initial and ultimate porosity of sediment as 0.523 and 0.355 (Swamee, 2001) and the values for future 25, 50, 75 and 100 years are computed by linear interpolation and are given in Table 5.5. The life of Pong reservoir is estimated as

330 years if the present rate of sedimentation continues (Swamee, 2001). L-moment ratios such as L-coefficient of variation (τ), L-skewness (τ_3) and L-kurtosis (τ_4) are used to fit Kappa distribution to yearly average unit weights of sediment computed from the particle size distribution of suspended sediment concentration Jwala Mukhi. The fitted Kappa distribution is used to generate 500 realizations of the unit weights of the sediment. The generated 500 realizations are used to fit any one of the three parameter distributions such as generalized logistic (*GLO*), Generalized extreme value (*GEV*), Generalized normal, Pearson type III and generalized Pareto for the purpose of quantile estimation. The goodness of fit estimate (z) for generalized logistic (*GLO*), Generalized extreme value (*GEV*), Generalized normal, Pearson type III and generalized Pareto distributions are -10.20, -10.77, -10.71, -10.75 and -11.89 respectively and desirable limit of z to declare the suitability of the distributions is less than or equal to ± 1.64 . It is found that none of the distributions considered are suitable and in this case Wakebey distribution is selected as the suitable distribution for explaining the unit weights of the sediment. The parameter estimates for Wakebey distribution are $\xi = 0.000$, $\alpha = 135.127$, $\beta = 136.913$, $\gamma = 0.009$ and $\delta = 0.541$ and the quantile estimates of unit weights of sediment for future 25, 50, 75 and 100 using the parameters are given Table 5.5.

Table 5.5. Consolidated unit weights of the sediment by different methods

Year	Consolidated unit weights of sediment (kg/m^3)			
	Particle size distribution	Porosity of uniform sediment	Hydrographic survey	Frequency Analysis
25 (2034)	1205.082	1338.250	1170.548	1239.541
50 (2059)	1216.336	1371.977	1181.802	1289.791
75 (2084)	1223.099	1405.705	1188.565	1329.206
100 (2109)	1227.959	1439.432	1193.425	1362.905

5.5 Prediction of Sediment Volume

The trap efficiency of the reservoir is computed by the equation (4.16) for future 25, 50, 75 and 100 years and is presented in Table 5.6. The sediment volumes are obtained by converting the sediment yield at Pong for 25, 50, 75 and 100 years using the corresponding consolidated unit weights of the sediment and trap efficiency and are presented in Table 5.7. The empirical formula proposed by Swamee (2001) is used to compute the volume of the sediment for future 25, 50, 75 and 100 years and is presented in Table 5.7.

Table 5.6. Trap efficiency of the reservoir by empirical formula

Year	Trap efficiency %
25 (2034)	100
50 (2059)	99
75 (2084)	98
100 (2109)	95

The consolidated sediment volume computed by hydrographic survey is considered to be the realistic since the unit weight of the sediment is computed from observed sediment load and the volume of the silt retained in the reservoir during 1987 to 2009. The sediment volumes computed by Empirical formula for future 25, 50, 75 and 100 years are 9.86%, 20.78%, 40.08% and 42.59% higher than the sediment volumes computed by hydrographic survey. The sediment volumes for higher prediction periods are much higher than the lower prediction periods. The sediment volumes computed by particle size distribution for future 25, 50, 75 and 100 years are 0.99%, 1.44%, 1.60% and 1.75% lower than the sediment volume computed by hydrographic survey. The sediment volumes computed by porosity of uniform sediment for future 25, 50, 75 and 100 years are 4.25%, 6.99%, 8.59% and 10.82% lower than the sediment volume computed by hydrographic survey. The sediment volumes computed by frequency analysis of particle size distribution for future 25, 50, 75 and 100 years are 1.88%, 4.19%, 5.90% and 7.86% lower than the sediment volume computed by hydrographic survey. The sediment volumes computed by particle size distribution for future 25, 50, 75 and 100 years are very close to sediment volumes computed by hydrographic survey. The comparison of results show that the sediment volume can be computed by consolidated unit weights of sediment by particle size distribution, porosity of uniformly distributed sediment and frequency analysis in the absence of data from hydrographic survey.

Table 5.7. Prediction of sediment volume by different methods

Year	Sediment volume (Mm ³)				
	Particle size Distribution	Porosity of uniform Sediment	Hydrographic survey	Frequency analysis	Empirical formula
25 (2034)	1287.867	1245.283	1300.683	1276.111	1428.970
50 (2059)	1693.419	1599.136	1718.135	1646.190	2075.230
75 (2084)	1907.018	1771.321	1937.880	1823.466	2714.610
100 (2109)	2302.040	2089.513	2343.153	2159.054	3341.130

5.6 Prediction of Elevation-Area-Capacity Curves

The sediment volumes computed by different methods as mentioned in the forgoing section are distributed in the reservoir by empirical area reduction method. The determination of the type of the reservoir is the first requirement to perform this computation. Two m values, 4.0 for lower elevations and 2.05 for the remaining portion of the reservoir, are obtained from the plot of depth V_s capacity on *log-log* paper. The *log-log* plot of depth V_s reservoir capacity is given in Figure 5.7. The mode of operation of the reservoir and the slope m which covers the most part of the reservoir suggest that the reservoir comes under type II. After 50 years of operation, the reservoir changes into type I. The zero elevations of the reservoir for above sediment volumes are determined by considering the types of reservoir as mentioned above. The depth to determine function values for sediment volumes computed for future 25, 50, 75 and 100 years are computed and are plotted on semi-log with design curves for all the four types of reservoir. It is observed that depth to determine function curves are not intercepted with the design curve of reservoir type I. So the depth to determine function curve (design curve for the reservoir) is determined by area increment method and it is plotted with the other curves. The relative depths at which the depth to determine function curves for sediment volumes are intercepted with design curve by area increment method are considered as the zero elevation of the reservoir and are presented in Table 5.8.

Table 5.8 Zero elevation of the reservoir for the sediment volumes computed by different methods of consolidated unit weights of sediment

Year	Zero elevation of the reservoir (relative depth)				
	Particle size distribution	Porosity of uniform Sediment	Hydrographic survey	Frequency analysis	Empirical formula
25 (2034)	0.230	0.225	0.233	0.230	0.240
50 (2059)	0.265	0.258	0.265	0.260	0.295
75 (2084)	0.283	0.273	0.283	0.275	0.348
100 (2109)	0.310	0.295	0.318	0.300	0.403

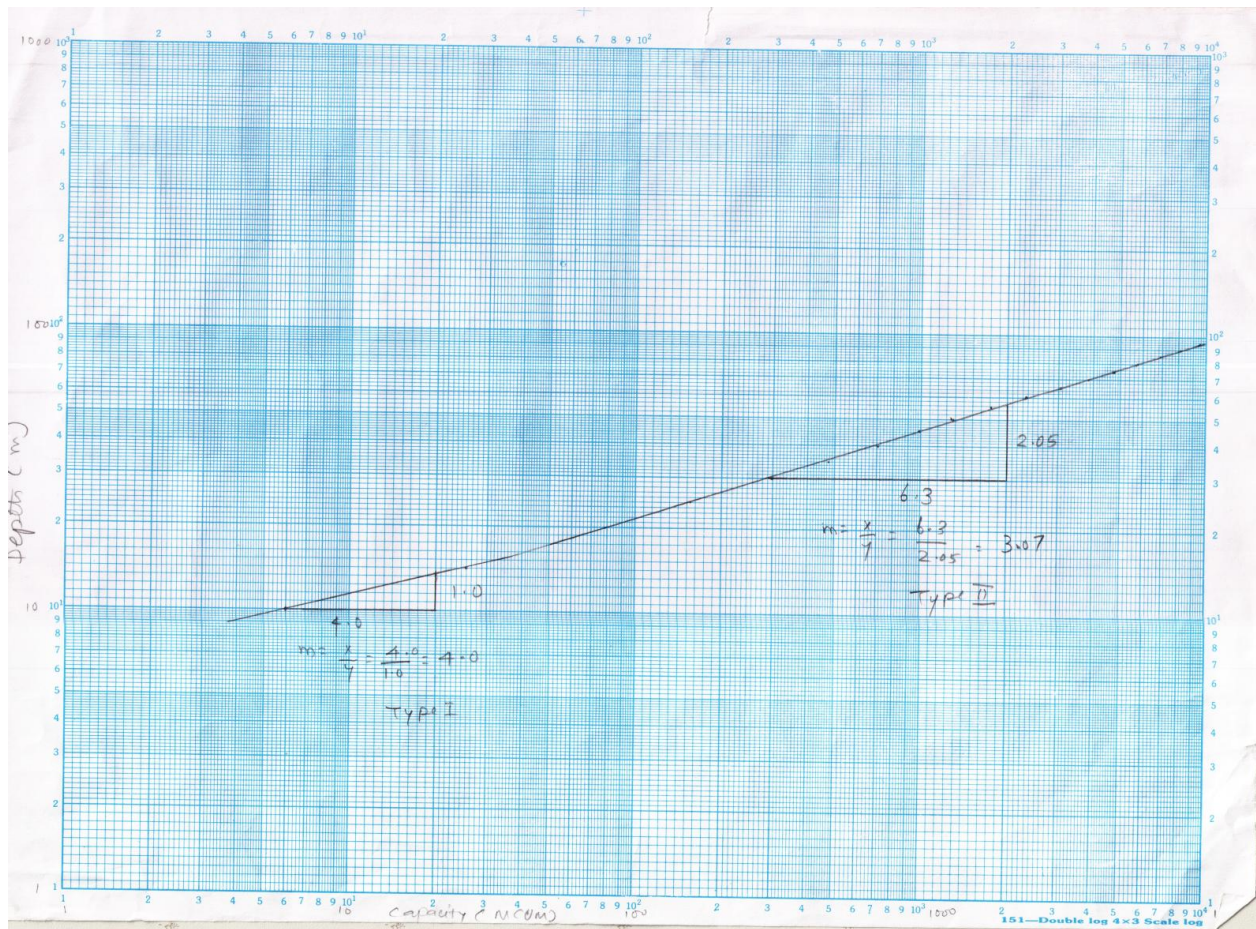


Figure 5.7 Depth Vs reservoir capacity

The zero elevation of the reservoir for the sediment volumes by different methods are given in Figures from 5.8 to 5.12.

The relative areas of sediment for the reservoir are computed from the equation of design area curve for type I reservoir. The constants K , proportionality for converting relative sediment areas to actual area, are computed and the reservoir area are computed by multiplying K with the relative area at each elevation of the reservoir. The sediment volumes at each elevation are computed by end area method. The computations are repeated till the sediment volume to be distributed in the reservoir is equal to the accumulated sediment volume at all elevation of the reservoir. The same procedure is adopted for the computation of reservoir area and capacity at each elevation for the sediment volumes computed by different methods. The number of iterations required to get the final distribution of sediment volume obtained by different methods are given Table 5.9. The reservoir area and capacity at elevation are deducted from the original reservoir area and capacity to get the revised reservoir area and capacity for future 25, 50, 75 and 100 years. The original reservoir area

and capacity curves are presented in Figure 5.13 respectively. The revised elevation-area-capacity curves derived for sediment volumes obtained by different methods are presented in Figures from 5.14 to 5.33. The percentages of reservoir capacity lost for the predicted sediment volumes for 25, 50, 75 and 100 are given in Table 5.10.

Table 5.9 Number of iterations to get the final distribution of sediment in the reservoir

Year	No of iterations				
	Particle size distribution	Porosity of uniform Sediment	Hydrographic survey	Frequency analysis	Empirical formula
25 (2034)	11	11	11	11	11
50 (2059)	12	11	12	11	12
75 (2084)	12	12	12	12	13
100 (2109)	12	12	13	12	15

From the above table it is observed that the number of iterations required to distribute the sediment volume for each prediction period is almost same.

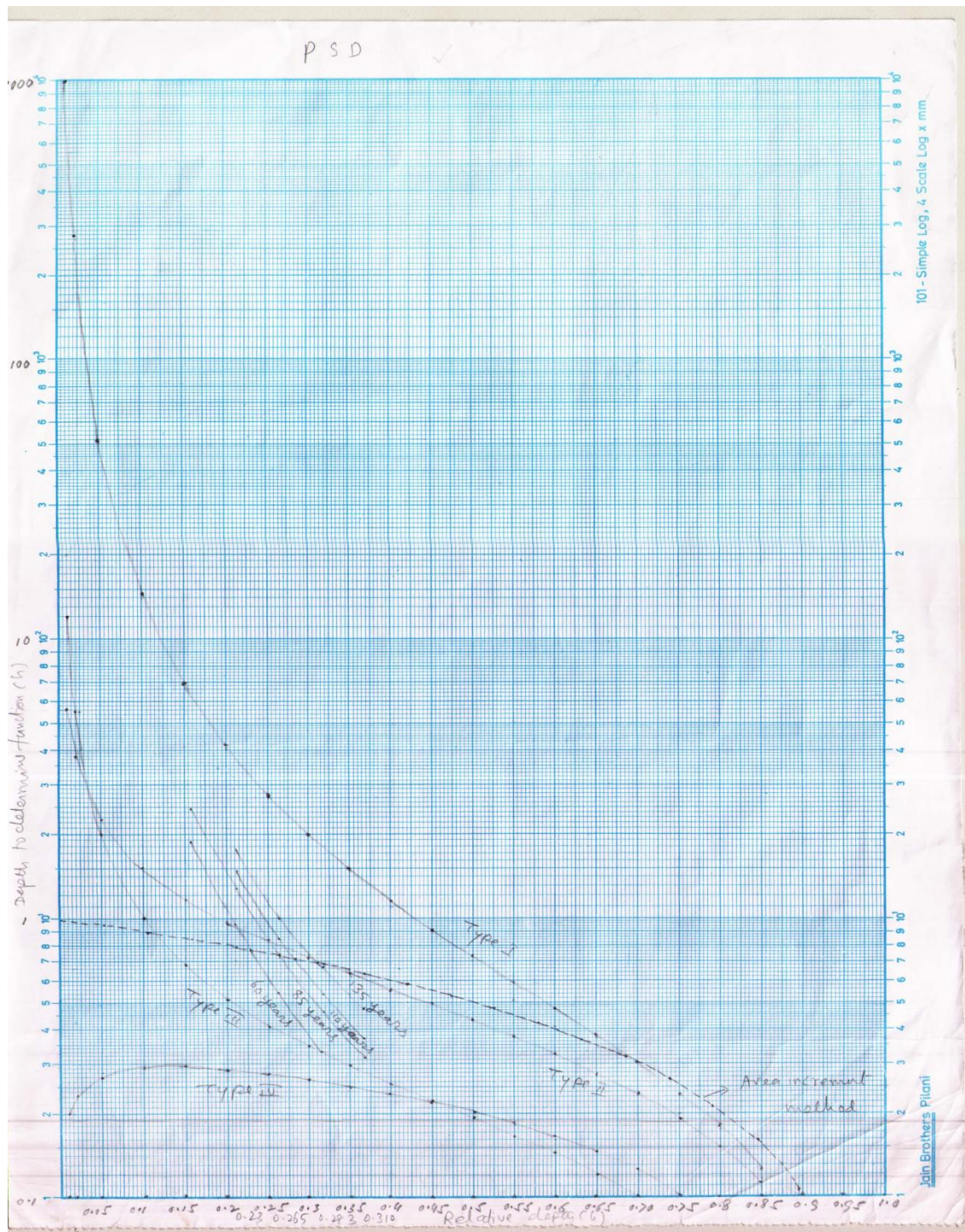


Figure 5.8 Determination of zero elevation of the reservoir for the sediment volumes of 25, 50, 75 and 100 years computed by the particle size distribution

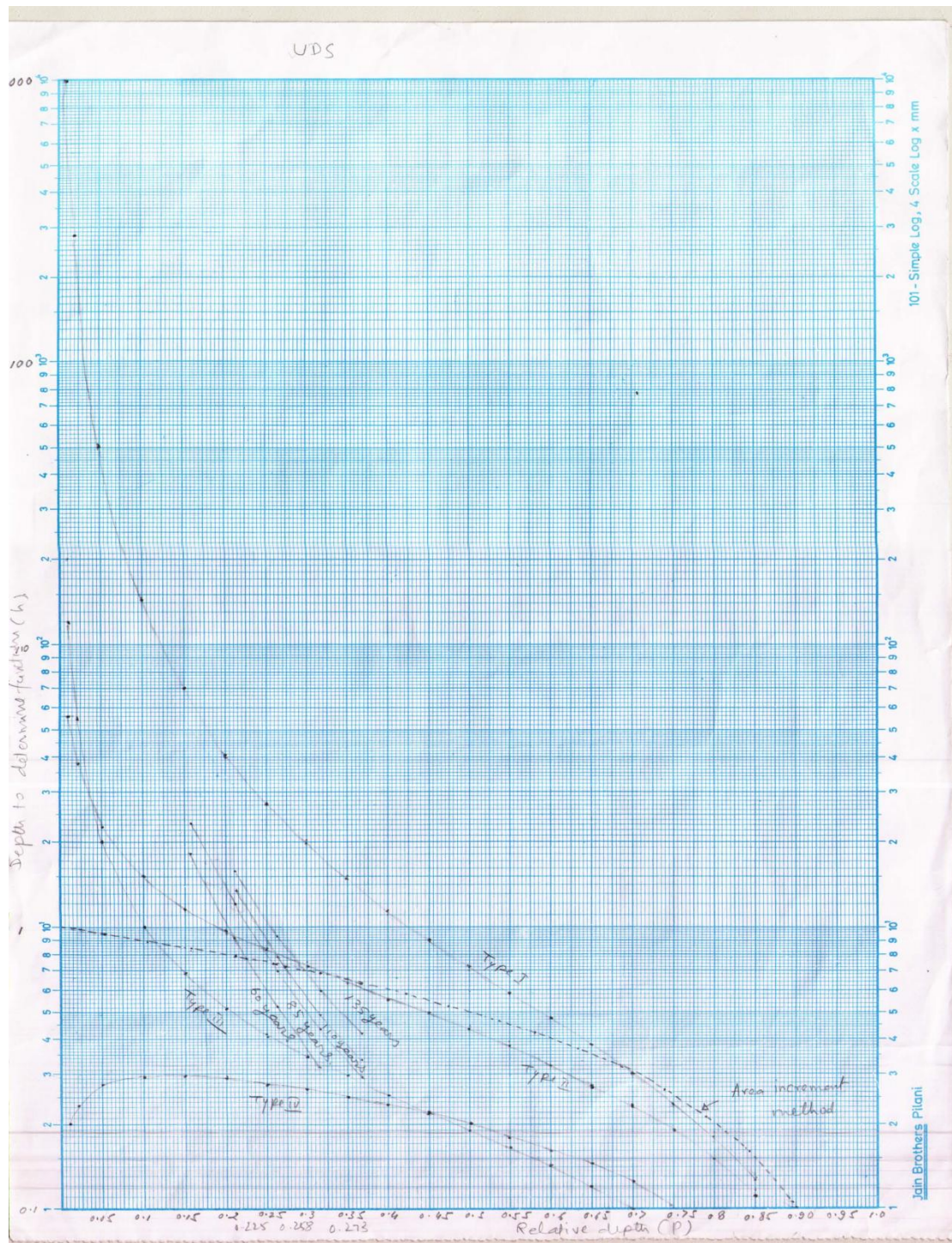


Figure 5.9 Determination of zero elevation of the reservoir for the sediment volumes of 25, 50, 75 and 100 years computed by the porosity of the uniform sediment

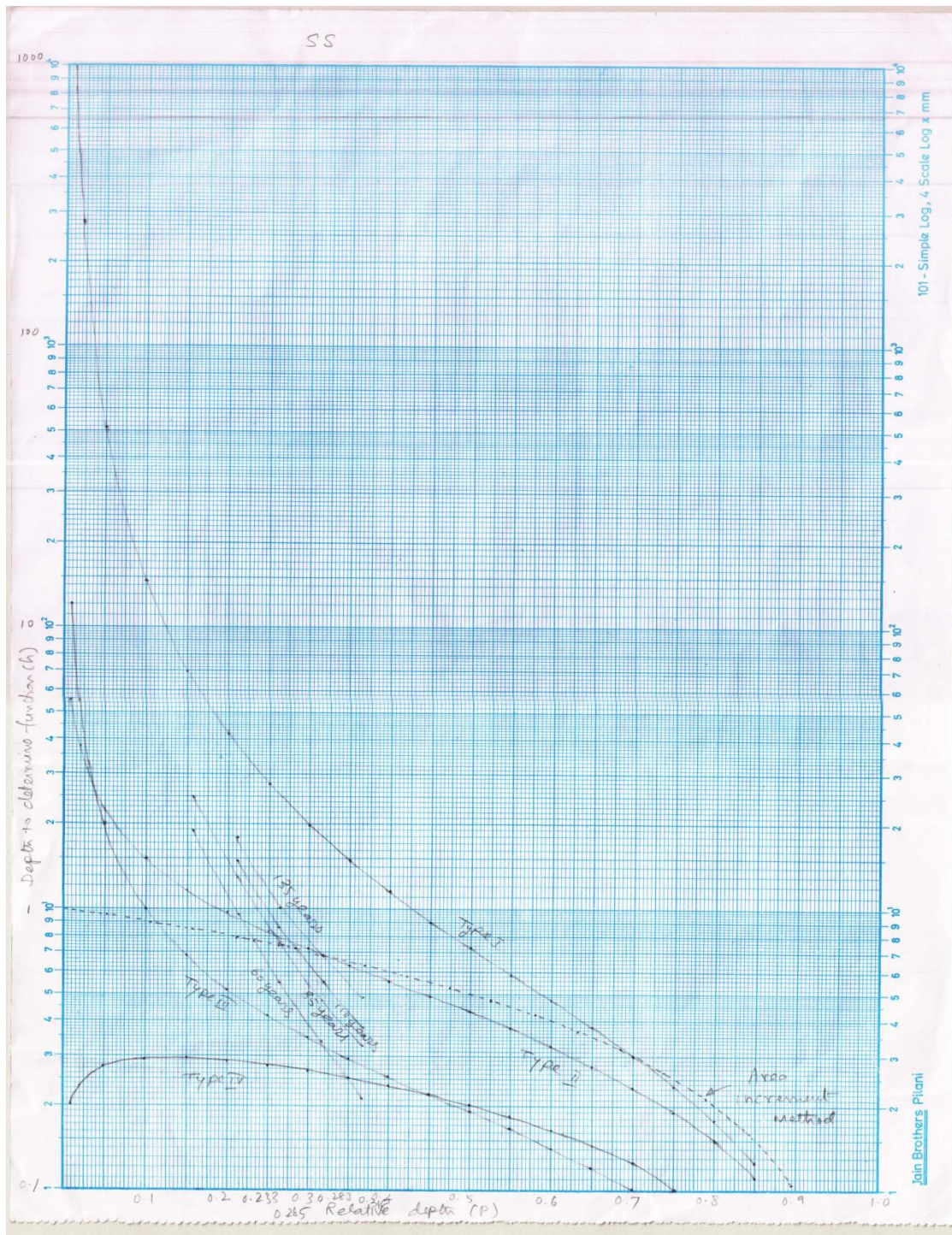


Figure 5.10 Determination of zero elevation of the reservoir for the sediment volumes of 25, 50, 75 and 100 years computed by the hydrographic survey

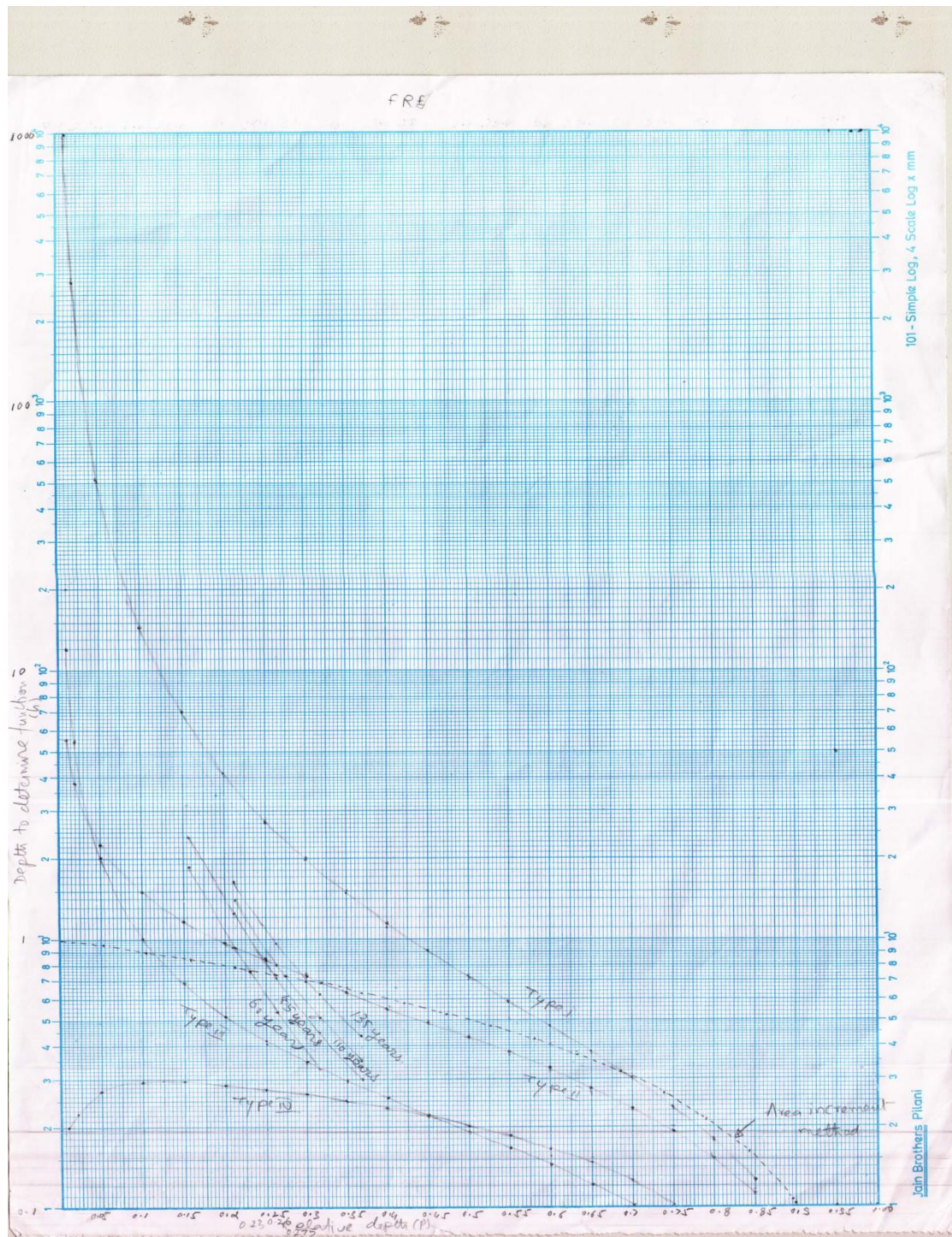


Figure 5.11 Determination of zero elevation of the reservoir for the sediment volumes of 25, 50, 75 and 100 years computed by the frequency analysis

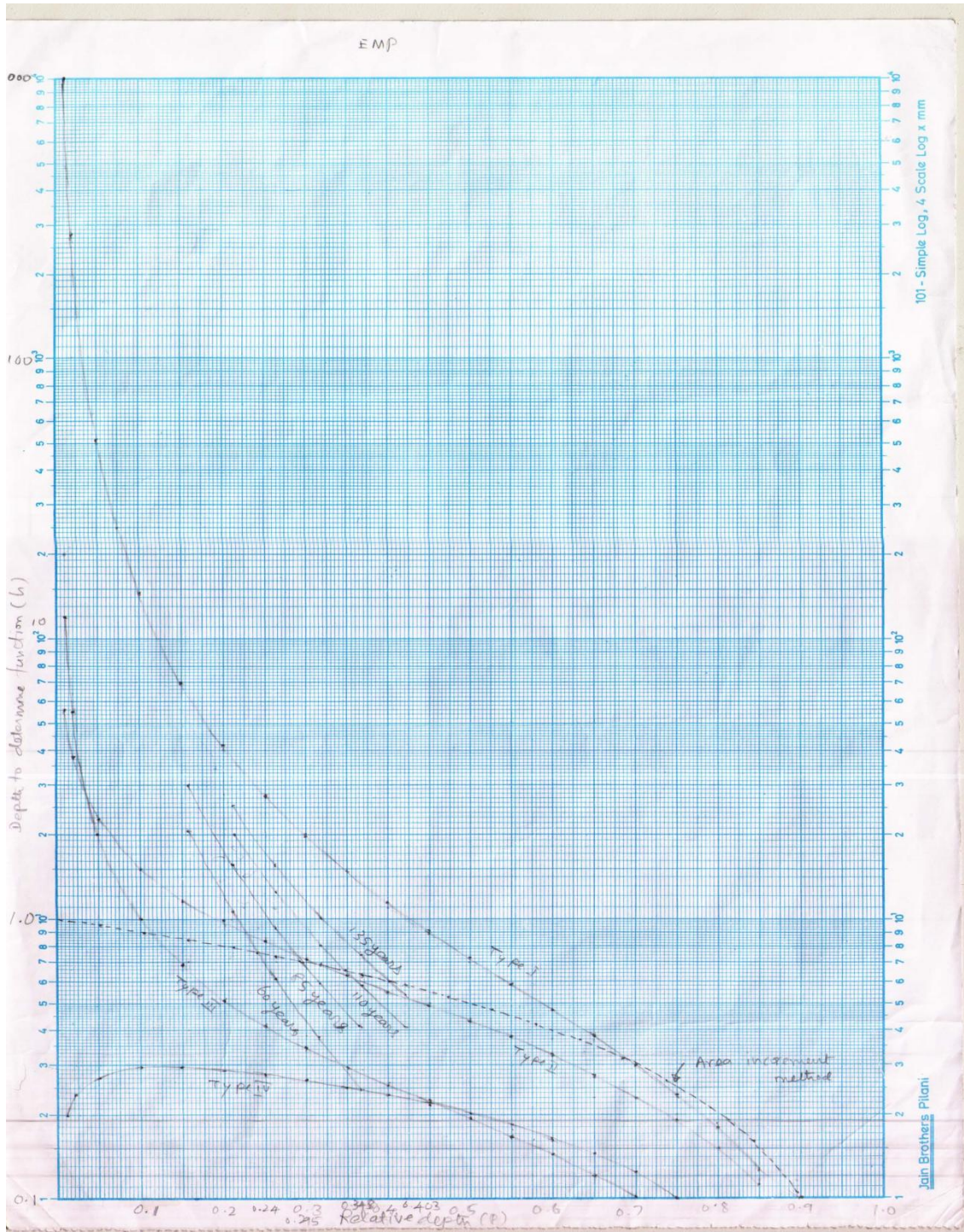


Figure 5.12 Determination of zero elevation of the reservoir for the sediment volumes of 25, 50, 75 and 100 years computed by the empirical formula

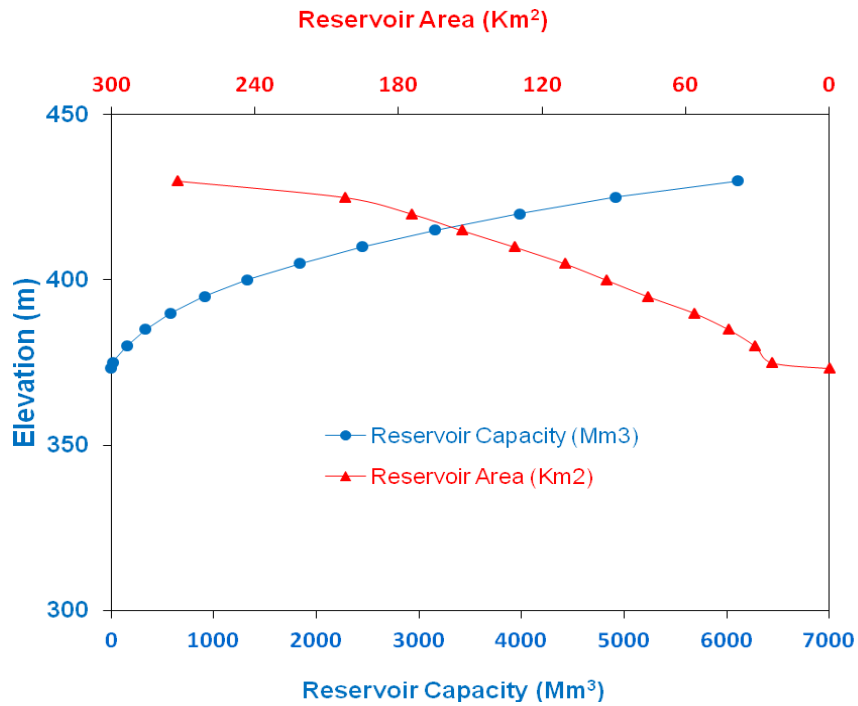


Figure 5.13 Original elevation-area-capacity curves

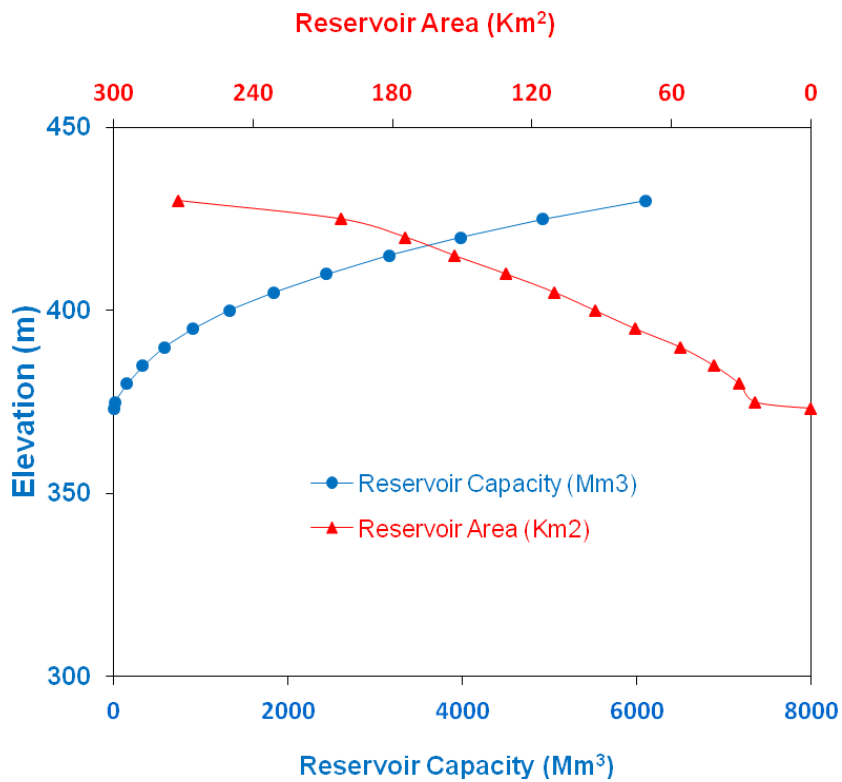


Figure 5.14 Elevation-area-capacity curves for sediment volume by empirical method after 25 years

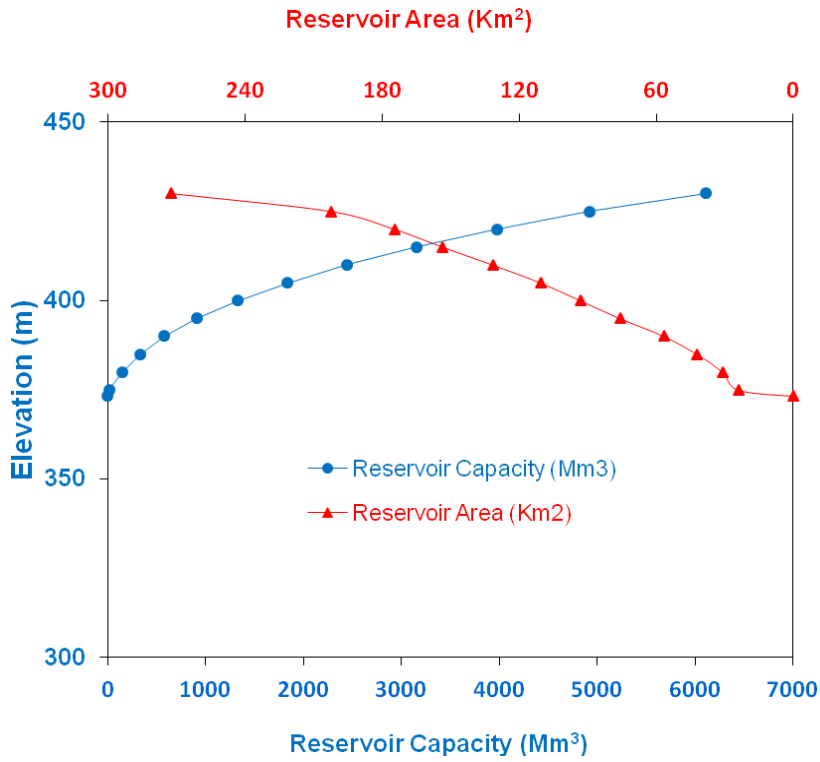


Figure 5.15 Elevation-area-capacity curves for sediment volume by empirical method after 50 years

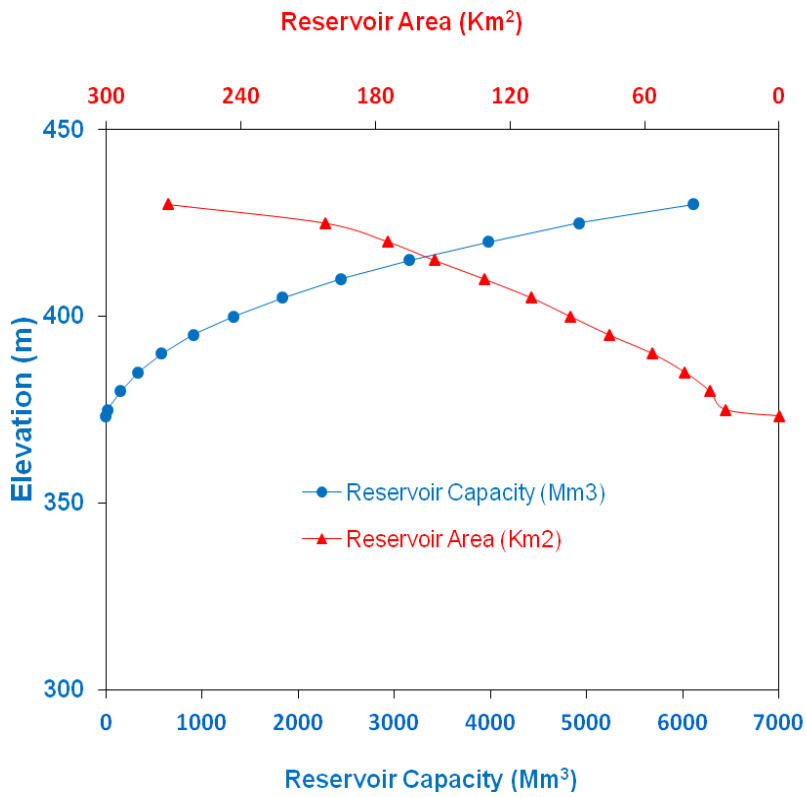


Figure 5.16 Elevation-area-capacity curves for sediment volume by empirical method after 75 years

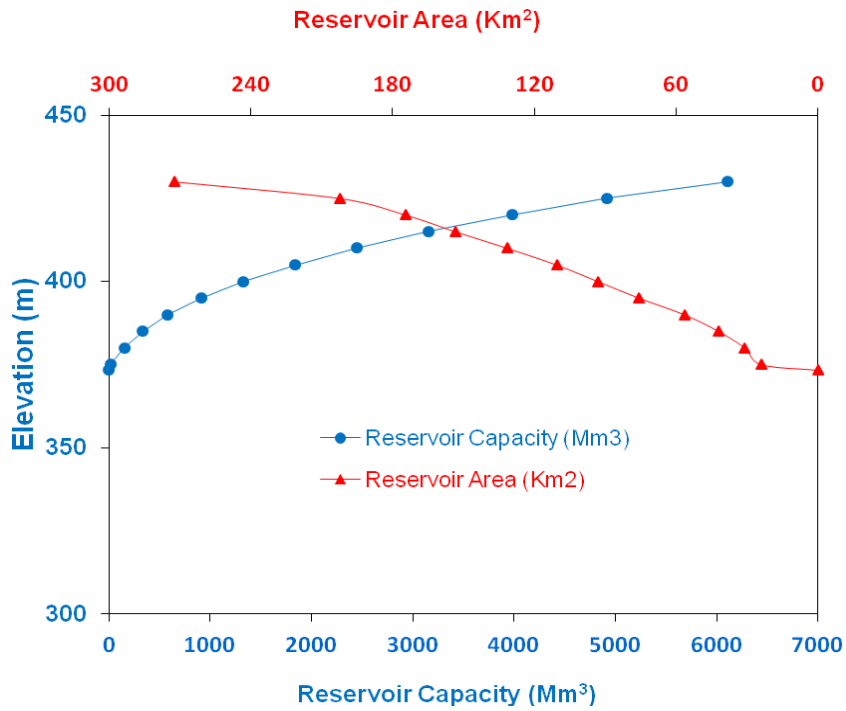


Figure 5.17 Elevation-area-capacity curves for sediment volume by empirical method after 100 years

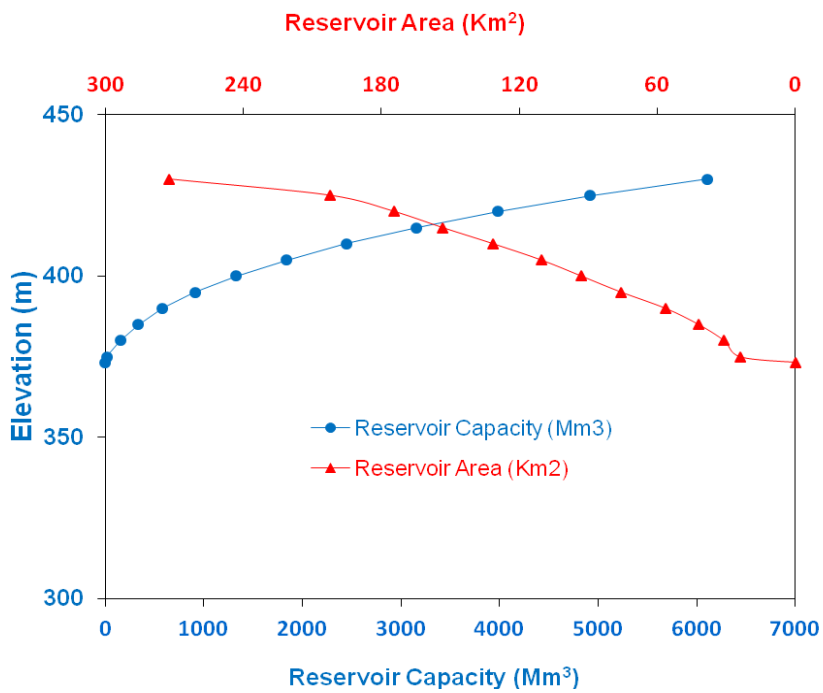


Figure 5.18 Elevation-area-capacity curves for sediment volume by frequency analysis after 25 years

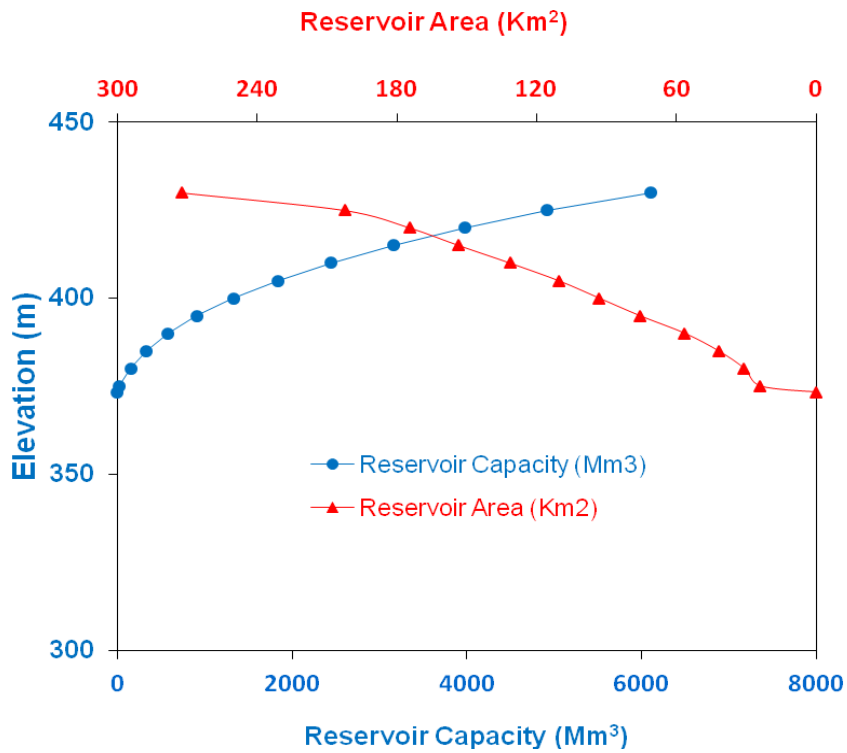


Figure 5.19 Elevation-area-capacity curves for sediment volume by frequency analysis after 50 years

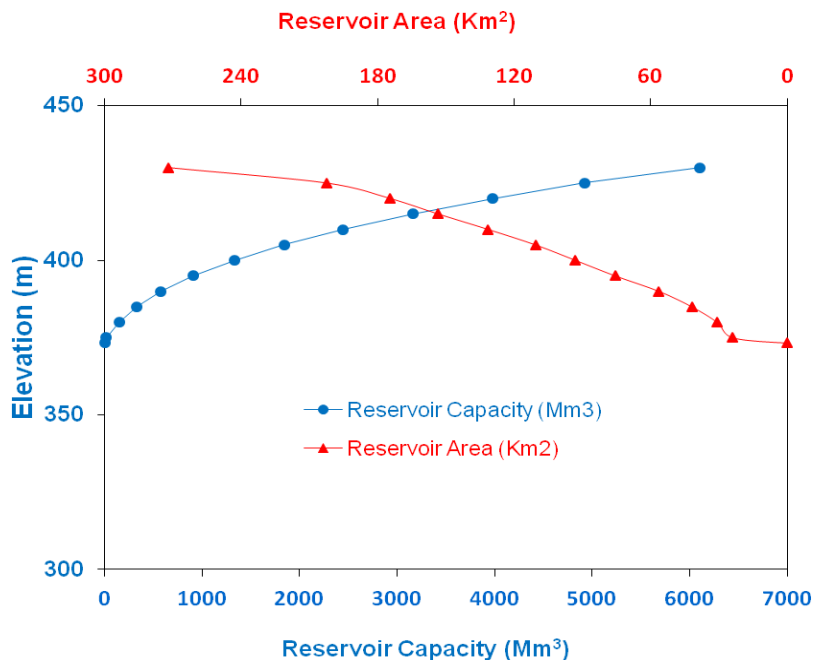


Figure 5.20 Elevation-area-capacity curves for sediment volume by frequency analysis after 75 years

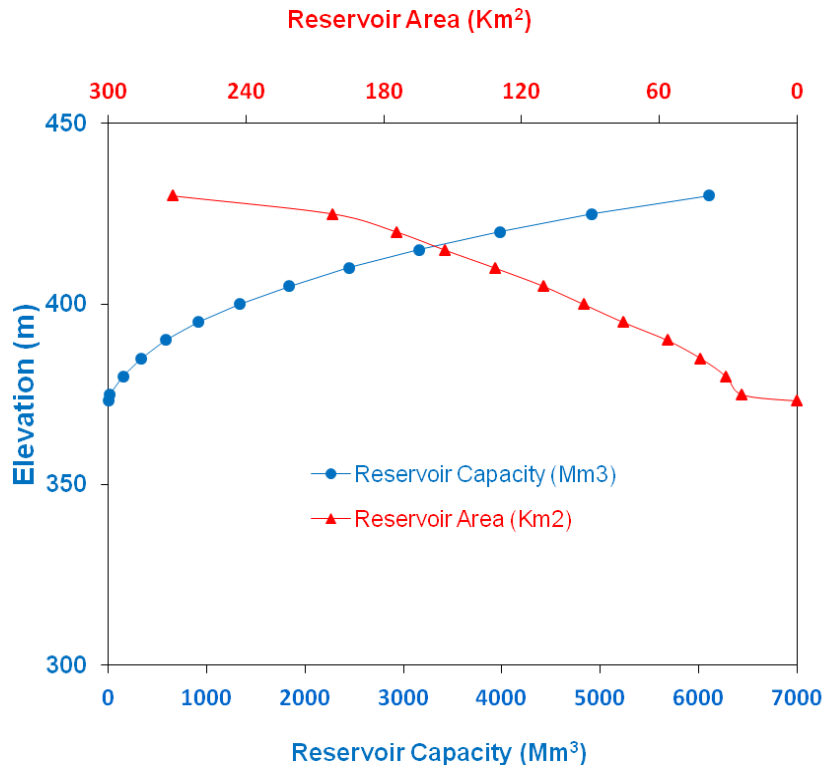


Figure 5.21 Elevation-area-capacity curves for sediment volume by frequency analysis after 100 years

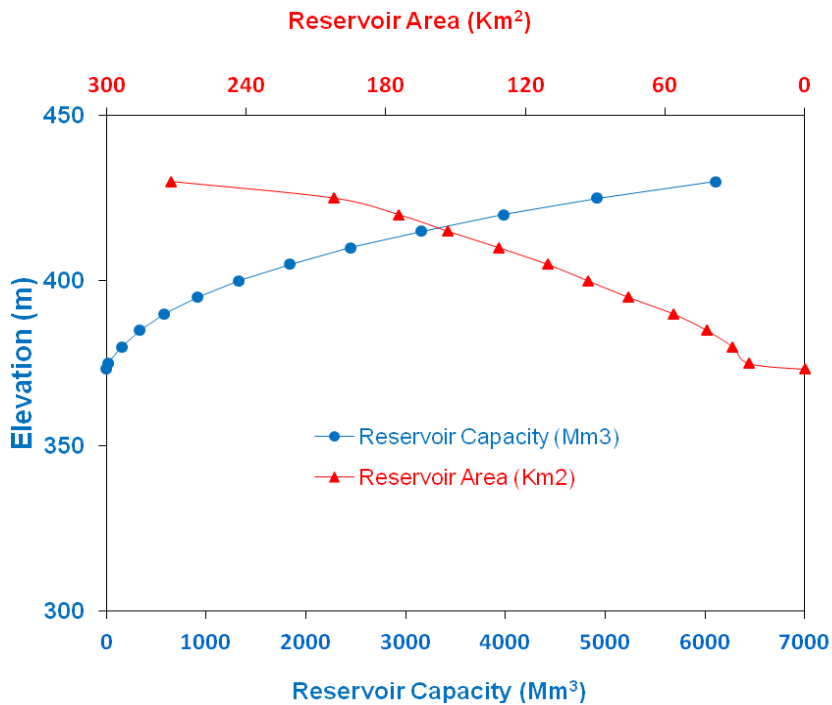


Figure 5.22 Elevation-area-capacity curves for sediment volume by particle size distribution after 25 years

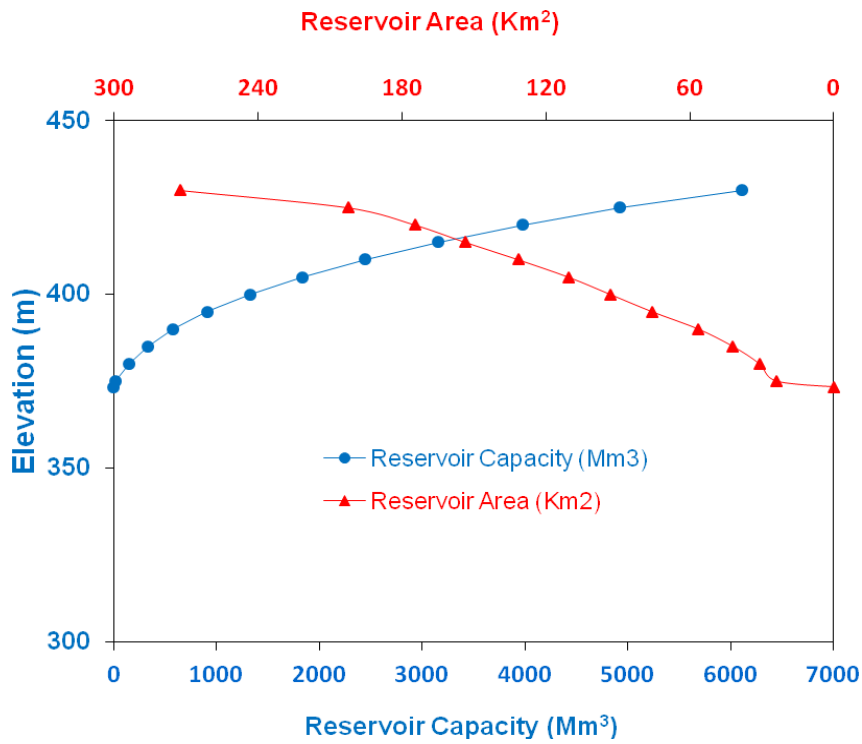


Figure 5.23 Elevation-area-capacity curves for sediment volume by particle size distribution after 50 years

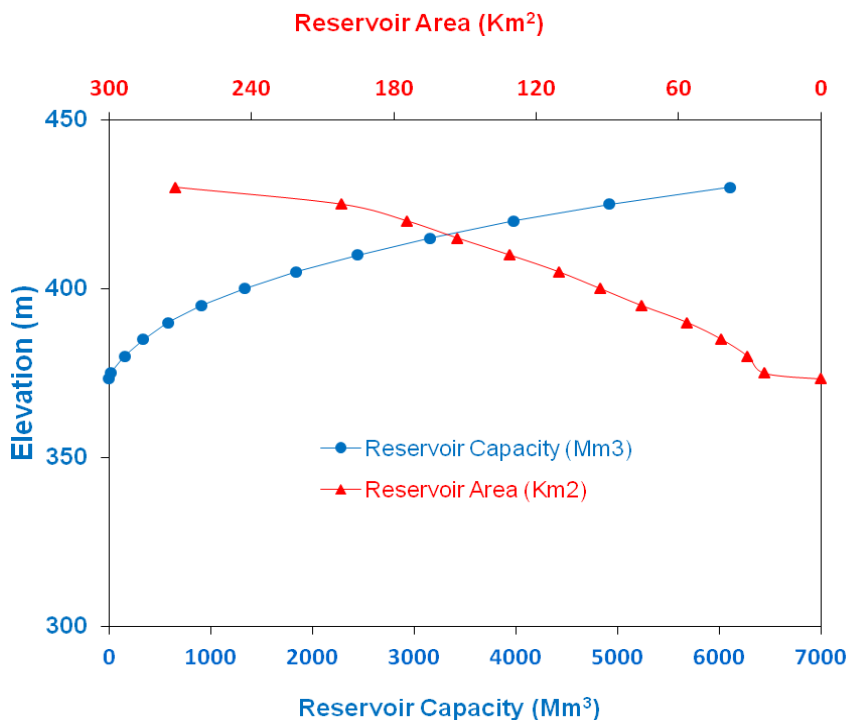


Figure 5.24 Elevation-area-capacity curves for sediment volume by particle size distribution after 75 years

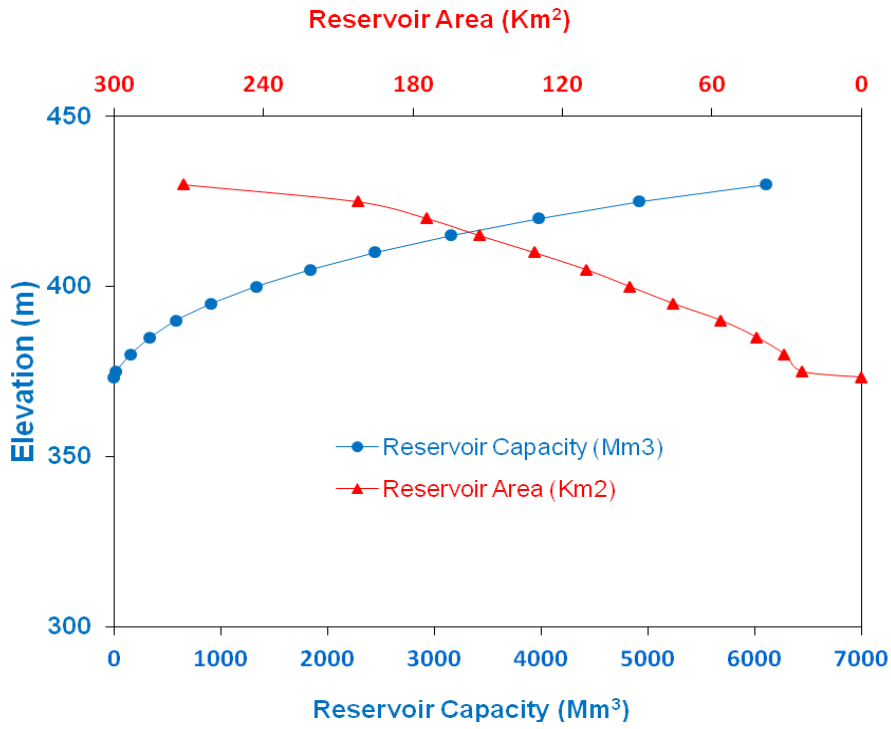


Figure 5.25 Elevation-area-capacity curves for sediment volume by particle size distribution after 100 years

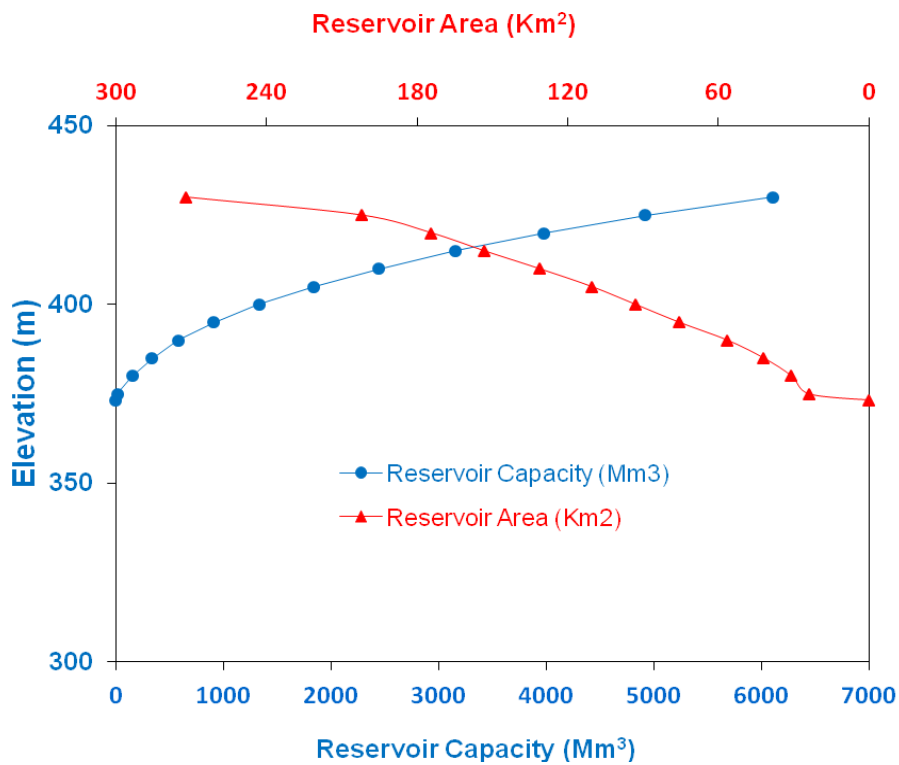


Figure 5.26 Elevation-area-capacity curves for sediment volume by hydrographic survey after 25 years

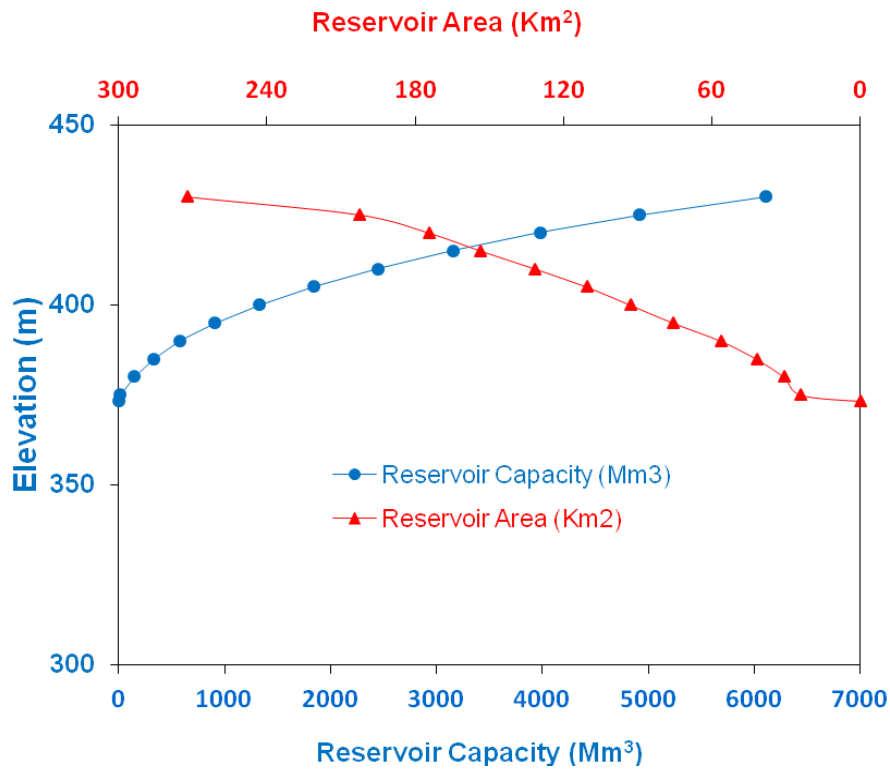


Figure 5.27 Elevation-area-capacity curves for sediment volume by hydrographic survey after 50 years

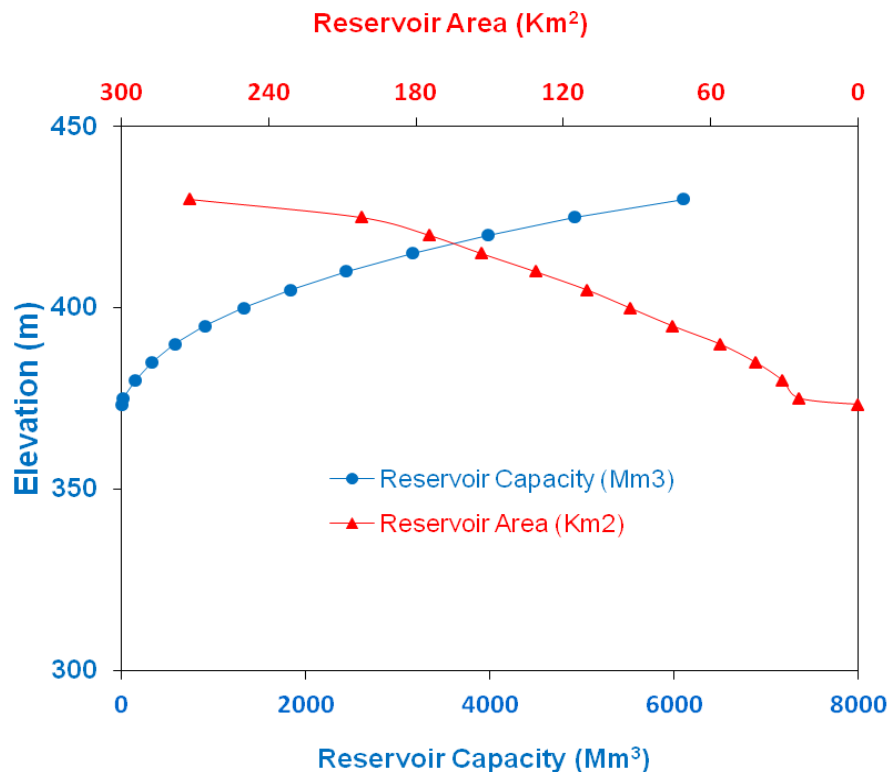


Figure 5.28 Elevation-area-capacity curves for sediment volume by hydrographic survey after 75 years

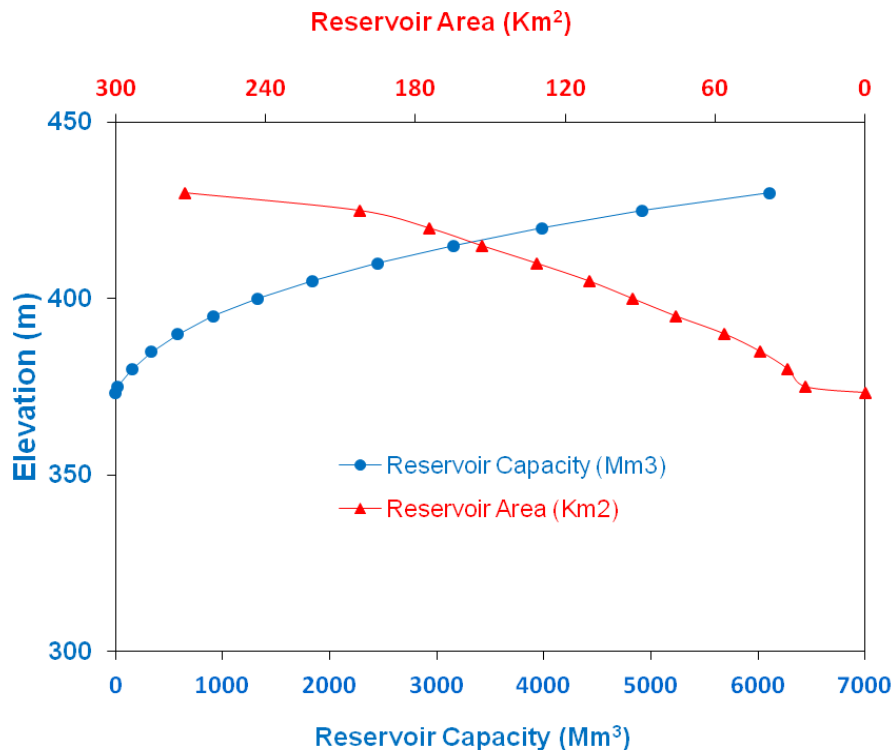


Figure 5.29 Elevation-area-capacity curves for sediment volume by hydrographic survey after 100 years

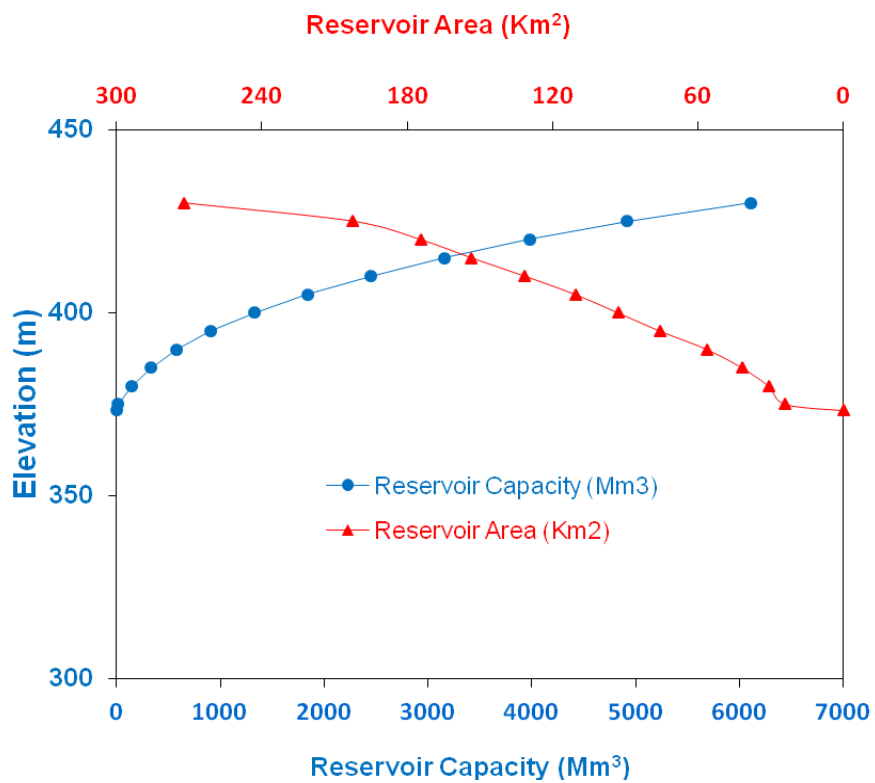


Figure 5.30 Elevation-area-capacity curves for sediment volume by porosity of uniform sediment after 25 years

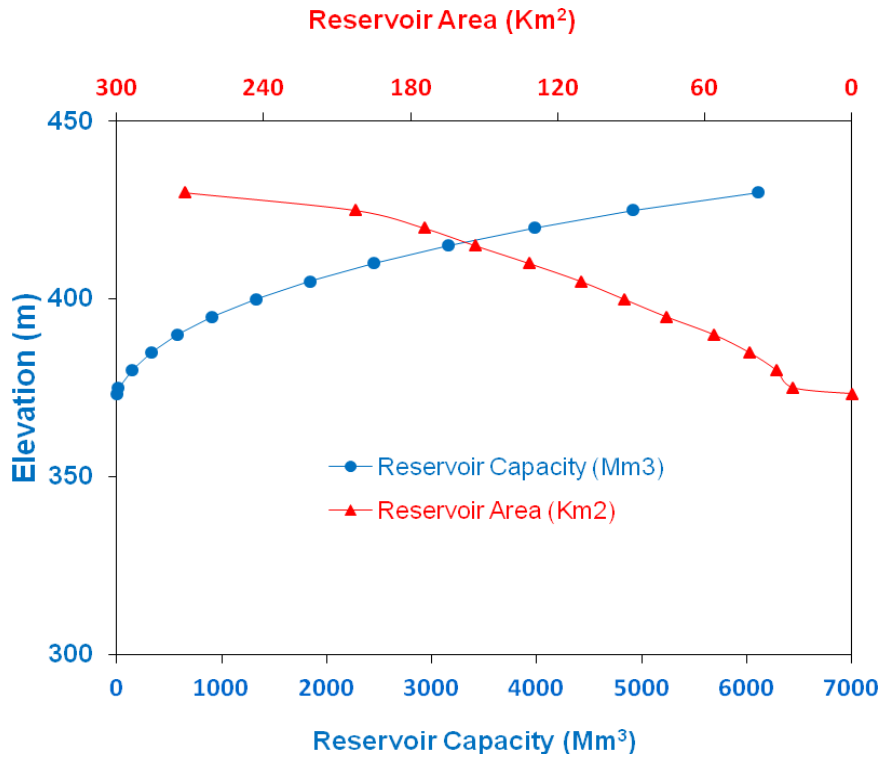


Figure 5.31 Elevation-area-capacity curves for sediment volume by porosity of uniform sediment after 50 years

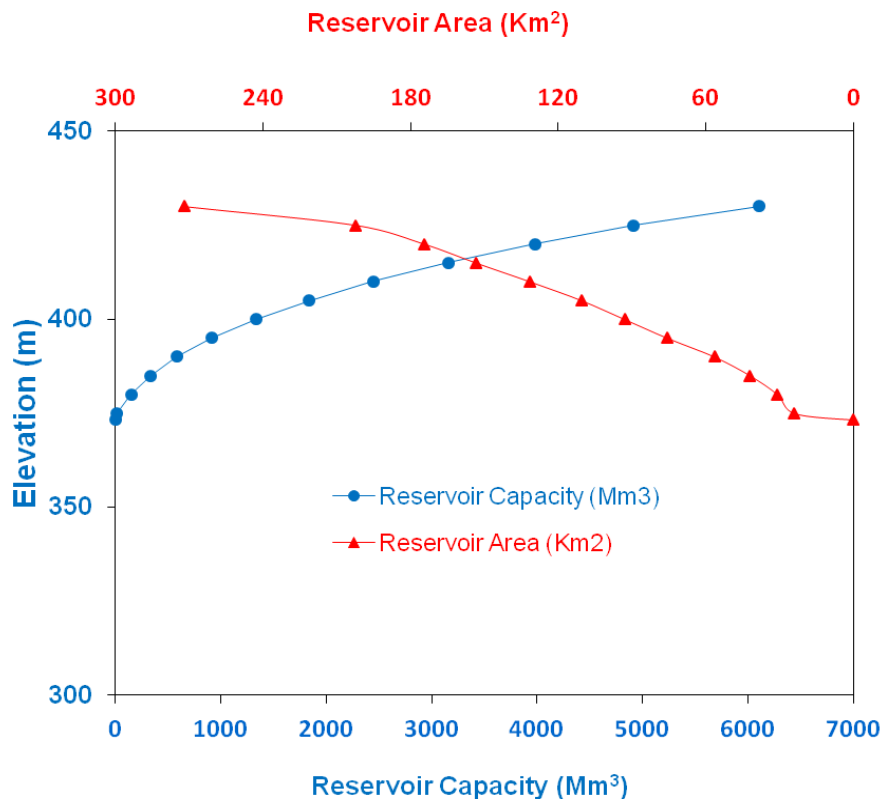


Figure 5.32 Elevation-area-capacity curves for sediment volume by porosity of uniform sediment after 75 years

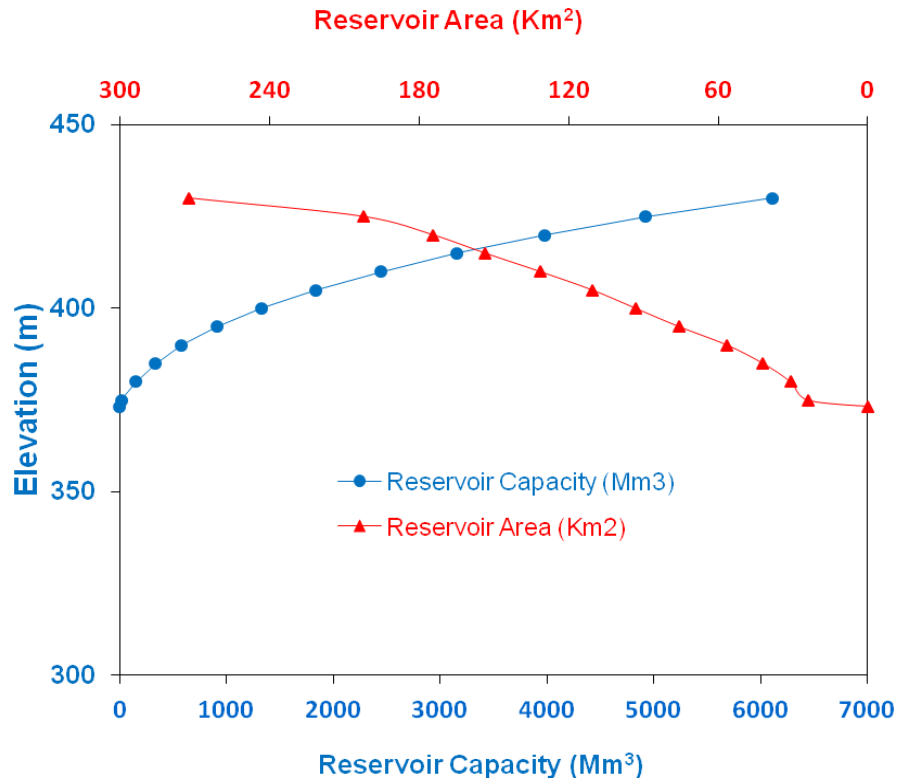


Figure 5.33 Elevation-area-capacity curves for sediment volume by porosity of uniform sediment after 100 years

Table 5.10 Percentage of reservoir capacity lost for sediment volume by different methods

Year	Percentage of reservoir capacity lost				
	Particle size distribution	Porosity of uniform Sediment	Hydrographic survey	Frequency analysis	Empirical formula
25 (2034)	15.01	14.52	15.16	14.87	16.66
50 (2059)	19.74	18.64	20.03	19.19	24.19
75 (2084)	22.23	20.65	22.59	21.26	31.64
100 (2109)	26.83	24.36	27.31	25.17	38.95

The percentages of reservoir capacity lost by different methods for the prediction period of 25 years vary from 14.52 % to 16.66%. The values for the prediction period of 50 years vary from 18.64% to 24.19%. The values for the prediction period of 75 years vary from 20.65% to 31.645%. The values for the prediction period of 100 years vary from 24.36 % to 38.95%. The variation in the percentages of reservoir capacity lost for

the prediction period of 25 and 50 years are low. The variation in the percentages of reservoir capacity lost for the prediction period of 75 and 100 years are high.

Chapter 6

Conclusions

The monthly rainfall at Dehra Gopipur, Haripur, Nangal Chowk and Pong dam and monthly flow volume and sediment yield at Jwala Mukhi from 1987 to 2009 are used to develop ANN model to simulate the sediment load. The feed forward ANN is trained with input vector selected from the available data. The monthly data from 1987 to 2007 are considered for the training of the model and data from 2008 to 2009 are considered for the validation of the model. The ANN model with input vector of flowvol(t), raindehra(t), rainhari(t), rainnangch(t), rainpondam(t) and the structure of 5-2-1 is the best model among the all. The monthly rainfall at Dehra Gopipur, Haripur, Nangal Chowk and Pong dam and monthly flow volume at Jwala Mukhi for future 25, 50, 75 and 100 years are generated by using time series modelling. The best ANN model is used to simulate the sediment load for future 25, 50, 75 and 100 years using the generated series of rainfall and flow volume.

The unit weights of deposited sediment in the reservoir are computed by different methods. The consolidated unit weights of the sediment are computed by the equation proposed by Miller of USBR. The consolidated unit weight is also obtained by frequency analysis of unit weights derived from particle size distribution. The consolidated unit weights obtained by different methods are used to compute the possible range of sediment volume expected to be deposited in the reservoir for the future 25, 50, 75 and 100 years. The elevation area capacity tables are revised for future 25, 50, 75 and 100 years by empirical area reduction method. The variation in the percentages of reservoir capacity lost for the prediction period of 25 and 50 years are low. The variation in the percentages of reservoir capacity lost for the prediction period of 75 and 100 years are high.

Chapter 7 References

1. ASCE Task Committee on Application of Artificial Neural Networks in Hydrology. (2000a). "Artificial neural networks in hydrology-I: Preliminary concepts." *J. Hydrol. Engrg.*, 5(2), 115-123.
2. ASCE Task Committee on Application of Artificial Neural Networks in Hydrology. (2000b). "Artificial neural networks in hydrology-II: Hydrologic applications." *J. Hydrol. Engrg.*, 5(2), 124-137.
3. Bevan, K.J., Lamb, R, Quinn, P.F., Romanowicz, R., and Freer, J. (1995). "TOPMODEL in V.P. Singh (Ed). Computer models of watershed hydrology." *Water Resources Publications*, 627-668.
4. Bhakra Beas Management Board (BBMB) (2003). *Sedimentation Studies: Period 2001-03*, Sedimentation Survey Report, Bhakra Dam Circle, BBMB, Nangal Township, Punjab, India.
5. Bhallamudi, S. M., and Chaudhry, M, H. (1991). "Numerical modelling of aggradation and degradation in alluvial rivers." *J. Hydr. Engrg.*, 117(9), 1145-1164.
6. Bhargava, D. N., Agarwal, C. K., Tyagi, S. S., and Verma, R. S. (1989). "Sedimentation of reservoirs in U. P." *Third International Workshop on Alluvial River Problems*, Oxford & IBH Publishing Co., New Delhi, 197-208.
7. Bhattacharjya, R. K., Datta, B., and Satish, M. G. (2007). "Artificial neural networks approximation of density dependent saltwater intrusion process in coastal aquifers." *J. Hydrol. Engrg.*, 12(3), 273-282.
8. Borland, W.M., and Miller, S. P. (1958). "Distribution of Sediment in large reservoirs." *Proc. ASCE*, 84(HY2).

9. Burian, S. J., Durrans, S.R., Nix, S. J., and Pitt, R.E. (2001). "Training artificial neural networks to perform rainfall disaggregation." *J. Hydrol. Engrg.*, 6(1), 43-50.
10. Central Water Commission (CWC). (2001). *Compendium on silting of reservoirs in India*, Water Planning and Projects Wing, Environment Management Organization, Watershed and Reservoir Sedimentation Directorate, CWC, New Delhi, India.
11. Chen, Y. H., Lopez, J. L., and Richarson, E. V. (1978). "Mathematical modelling of sediment deposition in reservoir." *J. Hydr. Div.*, 104, HY12, 1605-1616.
12. Chow, V.T., Maidment, D.R., and Mays, L.W. (1988). *Applied hydrology*, McGraw-Hill Book Company.
13. Cigizoglu, H. K. (2002). "Suspended sediment estimation for rivers using Artificial Neural Networks and Sediment Rating Curves." *Turkish J. Eng. Env. Sci.*, 26, 27-36.
14. Cigizoglu, H. K., and Kisi, O. (2006). "Methods to improve the neural network performance in suspended sediment estimation." *J. Hydrol.*, 317(3-4), 221-228.
15. Chitale, S. V., Sinha, S., and Misra, P. K. (1998). "Estimation of delta profile in the Indravati reservoir." *J. Hydr. Engg.*, 124(1), 109-113.
16. Cobaner, M., Unal, B., and Kisi, O. (2009). "Suspended sediment concentration estimation by an adaptive neuro-fuzzy and neural network approaches using hydro-meteorological data." *J. Hydrol.*, 367(1-2), 52-61.
17. Cornish, G., Bosworth, Perry, C., and Burke, J. (2004). *Water Charging in irrigated agriculture-An analysis of international experience*, FAO Water Reports no. 28, Food and Agriculture Organization of the United Nations, Rome.
18. Danh, N. T., Phien, H.N., and Gupta, A.D. (1999). "Neural network models for river flow forecasting." *Water SA*, 25(1), 33-39.

19. Danish Hydraulic Institute (1988). "Hydrological computerized modelling system (SHE)." Agern Alles, DK-2970 Horsholm, Denmark.
20. Dawson, C. W., and Wilby, R. (1998). "An artificial neural network approach to rainfall-runoff modeling." *Hydrol. Sci. J.*, 43(1), 47-66.
21. Deasy, C., Brazier, R. E., Heathwaite, A. L., and Hodgkinson, R. (2009). "Pathways of runoff and sediment transfer in small agricultural catchments." *Hydrolog. Process.*, 23(9), 1349-1358.
22. Deka, P., and Chandramouli, V. (2003). "A fuzzy neural network model for deriving the river stage-discharge relationship." *Hydrol. Sci. J.*, 48(2), 197-209.
23. Doomen, A. M. C., Wijma, E., Zwolsman, J. J. G., and Middelkoop, H. (2008). "Predicting suspended sediment concentrations in the Meuse River using a supply-based rating curve." *Hydrolog. Process.* 22(12), 1846-1856.
24. Dugan, H. A., Lamoureux, S. F., Lafreniere, M. J., and Lewis, T. (2009). "Hydrological and sediment yield response to summer rainfall in a small high arctic watershed." *Hydrolog. Process.*, 23(10), 1514-1526.
25. Focsa, V. (1980). "Sedimentation of Iron Gates reservoir on the Danube." *J. Hydr. Div.*, 106, HY10, 1659-1676.
26. Elshorbagy, A., Simonovic, S. P., and Panu, U.S. (2000). "Performance evaluation of artificial neural networks for runoff prediction." *J. Hydrol. Engrg.*, 5(4), 424-427.
27. Fernando, A.K. and Jayawardena, A.W. (1998). "Runoff forecasting using RBF networks with OLS algorithm." *J. Hydrol. Engrg.*, 3(3), 203-209.
28. Fernando, D. A. K., and Shamseldin, A. Y. (2009). "Investigation of internal functioning of the radial-basis-function neural network river flow forecasting models." *J. Hydrol. Engrg.*, 14(3), 286-292.

29. Gao, P., and Pasternack, G. (2007). "Dynamics of suspended sediment transport at field-scale drain channels of irrigation-dominated watersheds in the Sonoran Desert, southeastern California." *Hydrolog. Process.*, 21(16), 2081-2092.
30. Garde, R. J., and Rangaraju, K. G. (1985). *Mechanics of sediment transportation and alluvial stream problems*, Wiley Eastern Limited, New Delhi.
31. Gill, M. K., Asefa, T., Kaheil, Y., and Mckee, M. (2007). "Effect of missing data on performance of learning algorithms for hydrologic predictions: Implications to an imputation technique." *Water Resour. Res.*, 43, W07416, 1-12.
32. Goel, N.K. (2003). *Stochastic hydrology-Lecture notes*, Department of Hydrology, Indian Institute of Technology, Roorkee, 247667
33. Govindaraju, R. S., and Rao, A. R. (2000). *Artificial neural networks in hydrology*, Kluwer Academic, Dordrecht, The Netherlands.
34. Graf, W. H. (1984). *Hydraulics of sediment transport*, Water Resources Publications, P.O. Box 2481, Littleton, Colorado 80161, U.S.A.
35. Hosking, J. R. M., and Wallis, J. R. (1997). *Regional frequency analysis: An approach based on L-moments*, Cambridge University Press, The Edinburgh Building, Cambridge CB2 2RU, United Kingdom.
36. Horowitz, A.J., Elrick, K. A., and Smith, J. J. (2008). "Monitoring urban impacts on suspended sediment, trace element, and nutrient fluxes within the city of Atlanta, Georgia, USA: program design, methodological considerations, and initial results." *Hydrolog. Process.*, 22(10), 1473-1496.
37. Hsu, K-L., Gupta, H.V., and Sorooshian, S. (1995). "Artificial neural network modeling of the rainfall-runoff process." *Water Resour. Res.*, 31(10), 2517-2530.

38. Imrie, C.E., Durucan, S., and Korre, A. (2000). "River flow prediction using artificial neural networks: generalization beyond the calibration range." *J. Hydrol.*, 233(1-4), 138-153.
39. Ilich, N. (2008). "Shortcomings of linear programming in optimizing river basin allocation." *Water Resour. Res.*, 44, W02426, 1-14.
40. Jain, A., and Srinivasulu, S. (2004). "Development of effective and efficient rainfall-runoff models using integration of deterministic, real-coded genetic algorithms and artificial neural network techniques." *Water Resour. Res.*, 40, W04302, 1-12.
41. Jain, S.K., Das, A., and Srivastava, D.K. (1999). "Application of ANN for reservoir inflow prediction and operation." *J. Water Resour. Plann. Manage.*, 125(5), 263-271.
42. Jain, S. K. (2001). "Development of integrated sediment curves using ANNs " *J. Hydr. Engrg.*, 127(1), 30-37.
43. Jain, S. K. (2008). "Development of integrated discharge and sediment rating relation using a Compound Neural Network." *J. Hydrol. Engrg.*, 13(3), 124-131.
44. Jain, S. K., Singh, V. P., and Genuchten, M. T. V. (2004). "Analysis of soil water retention data using Artificial Neural Networks." *J. Hydrol. Engrg.*, 9(5), 415-420.
45. Jothiprakash, V., and Garg, V. (2009). "Reservoir Sedimentation Estimation using Artificial Neural Networks." *J. Hydrol. Engrg.*, 14(9), 1035-1040.
46. Kalteh, A. M., and Berndtsson, R. (2007). "Interpolating monthly precipitation by self organizing map (SOM) and multilayer perceptron (MLP)." *Hydrol. Sci. J.*, 52(2), 305-317.
47. Kasiviswanathan, K.S., Cibin, R., Sudheer, K.P., and Chaubey, I. (2013). "Constructing prediction interval for artificial neural network rainfall runoff models based on ensemble simulations." *J. Hydrol.*, 499, 275-288.

48. Kerssens, P. M. J., Prins, A., and Rijn, L. C. V. (1979). "Model for suspended sediment transport." *J. Hydr. Div.*, 105(5), 461-476.
49. Keskin, M. E., and Terzi, O. (2006). "Artificial neural network models of daily pan evaporation." *J. Hydrol. Engrg.*, 11(1), 65-70.
50. Kido, D., Chikita, K. A., and Hirayama, K. (2007). "Subglacial drainage system changes of the Gulkana Glacier, Alaska: discharge and sediment load observations and modelling." *Hydrolog. Process.*, 21(3), 399-410.
51. Kisi, O. (2004). "Multi-Layer perceptrons with Levenberg-Marquardt training algorithm for suspended sediment concentration prediction and estimation." *Hydrol. Sci. J.*, 49(6), 1025-1040.
52. Kisi, O. (2005). "Suspended sediment estimation using neuro-fuzzy and neural network approaches." *Hydrol. Sci. J.*, 50(4), 683-696.
53. Kisi, O. (2007). "Streamflow forecasting using different artificial neural network algorithms." *J. Hydrol. Engrg.*, 12(5), 532-539.
54. Lohani, A. K., Goel, N. K., and Bhatia, K. K. S. (2007). "Deriving stage-discharge-sediment concentration relationships using Fuzzy logic." *Hydrol. Sci. J.*, 52(4), 793-807.
55. Maier, H.R., and Dandy, G.C. (2000). "Neural networks for the prediction and forecasting of water resources variables: A review of modelling Issues and applications." *Environmental Modelling & Software*, 15, 101-124.
56. Mano, V., Nemery, J., Belleudy, P., and Poirel, A. (2009). "Assessment of suspended sediment transport in four alpine watersheds (France): influence of the climate regime." *Hydrolog. Process.*, 23(5), 777-792.

57. Minns, A. W., and Hall, M. J. (1996). "Artificial neural networks as rainfall runoff models." *Hydrol. Sci. J.*, 41(3), 399-417.
58. Miller, C. R. (1953). "Determination of the unit weight of sediment for use in sediment volume computations." U. S. Bureau of Reclamation, Denver.
59. Miraki, G. D. (1983). *Sediment yield and deposition profiles in reservoirs*, Ph.D. Thesis, Civil Engg. Deptt., University of Roorkee, Roorkee.
60. Molanezhad, M. (1984). *Mathematical Approach to reservoir sedimentation*, Ph.D. Thesis, Civil Engg. Deptt., University of Roorkee, Roorkee.
61. Morris, G. L., and Fan, J. (1997). *Reservoir sedimentation handbook – Design and Management of Dams, Reservoirs, and Watersheds for Sustainable Use*, McGraw-Hill, New Delhi.
62. Murthy, B. N. (1977). *Life of reservoir*, Technical Report no. 19, Central Board of Irrigation and Power, New Delhi-110001.
63. Nagesh Kumar, D., Srinivasa Raju, K., and Sathish, T. (2004). "River Flow Forecasting using Recurrent Neural Networks", *Water Resour. Manage.*, 18(2), 143-161.
64. Nagle, G. N., Fahey, T. J., Ritchie, J. C., and Woodbury, P.B. (2007). "Variations in sediment sources and yields in the Finger Lakes and Catskills regions of New York." *Hydrolog. Process.* 21(6), 828-838.
65. Nagy, H. M., Watanabe, K., and Hirano, M. (2002). "Prediction of sediment load concentration in rivers using artificial neural networks." *J. Hydr. Engrg.*, 128(6), 588-595.
66. Nash, J. E., and Sutcliffe, J. V. (1970). "River flow forecasting through conceptual models:1. A discussion of principles." *J. Hydrol.*, 10(3), 282-290.

67. Neitsch, S. L., Arnold, J.G., Kiniry, J. R., and Williams J. R. (2005). *Soil and Water Assessment Tool Theoretical Documentation – Version 2005*, Grassland, Soil and Water Research Laboratory, Agricultural Research Service, 808 East Blackland Road, Temple, Texas 76502.
68. Ojha, C. S. P., Berndtsson, R., and Bhunya, P. (2008). *Engineering hydrology*, Oxford University Press, YMCA Library Building, Jai Singh Road, New Delhi 110001.
69. Okabe, T., Amou, S., and Ishigaki, M. (1993). “A simulation model for sedimentation process in gorge type reservoirs.” *Sediment Problems: Strategies for Monitoring, Prediction and Control (Proceedings of the Yokohama Symposium, July 1993)*, IAHS Publ. No. 217,119-126.
70. Pandey, A., Chowdhary, V. M., Mal, B. C., and Billib, M. (2009). “Application of the WEPP model for prioritization and evaluation of best management practices in an Indian watershed.” *Hydrolog. Process.* 23(), 2997-3005.
71. Papanicolaou, A, N., Elahakeem, M., Krallis, G., Prakash, S., and Edinger, J. (2008). “Sediment transport modelling review-Current and Future developments.” *J. Hydr. Engrg.*, 134(1), 1-14.
72. Parajuli, P. B., Nelson, N. O., Frees, L. D., and Mankin, K. R. (2009). “Comparison of AnnAGNPS and SWAT model simulation results in USDA-CEAP agricultural watersheds in south-central Kansas.” *Hydrolog. Precess.* 23(5), 748-763.
73. Parasuraman, K., Elshorbagy, A., and Carey, S. K. (2006). “Spiking modular neural networks: A neural network modeling approach for hydrological processes.” *Water Resour. Res.* 42, W05412, 1-14.
74. Raghuwanshi, N. S., Singh, R., and Reddy, L. S. (2006). “Runoff and sediment yield modelling using Artificial Neural Networks: Upper Siwane River, India.” *J. Hydrol. Engrg.*, 11(1), 71-79.

75. Raman, H., and Chandramouli, V. (1996). "Deriving a general operating policy for reservoirs using Neural Network." *J. Water Resour. Plann. Manage.*, 122(5), 342-347.
76. Raman, H., and Sunilkumar, N. (1995). "Multivariate modelling of water resources time series using artificial neural networks." *Hydrol. Sci. J.*, 40(2), 145-163.
77. Rijn, L. C. (1984a). "Sediment transport, Part I: Bed load transport." *J. Hydr. Engrg.*, 110(10), 1431-1456.
78. Rijn, L. C. (1984b). "Sediment transport, Part II: Suspended load transport." *J. Hydr. Engrg.*, 110(11), 1613-1641.
79. Rijn, L. C. (1984c). "Sediment transport, Part III: Bed forms and alluvial roughness." *J. Hydr. Engrg.*, 110(12), 1733-1754.
80. Rumelhart, D., E., Hinton, E., and Williams, J. (1986). *Learning internal representation by error propagation, Parallel Distributed Processing, Vol. 1*, MIT Press, Cambridge, Mass., 318-362.
81. Sajikumar, S., and Thandaveswara, B.S. (1999). "A non-linear rainfall-runoff model using an artificial neural network." *J. Hydrol.*, 216(1-2), 32-55.
82. Salas, J. D., Delleur, J. W., Yevjevich, V. and Lane, W. L. (1980). *Applied modelling of hydrologic time series*, Water Resources Publications, P.O. Box 2841, Littleton, Colorado 80161, U.S.A.
83. Schwab, G. O., Fangmeier, D. D., Elliot, W. J., and Frevert, R. K. (1993). *Soil and water conservation engineering*, John Wiley & Sons, Inc, New York.
84. Shahin, M. M. A. (1993). "An overview of reservoir sedimentation in some African river basins." *Sediment Problems: Strategies for Monitoring, Prediction and Control (Proceedings of the Yokohama Symposium, July 1993)*, IAHS Publ. No. 217, 93-100.

85. Singh, V. P., and Regl, R. R. (1983). "Analytical solutions of kinematic equations for erosion on plane I. Rainfall of indefinite duration." *Adv. Water Res.*, 6, 2-10.
86. Singh, V. P. (1983). "Analytical solutions of kinematic equations for erosion on plane II. Rainfall of definite duration." *Adv. Water Res.*, 6, 88-95.
87. Singh, V. P., and Tayfur, G. (2008). "Kinematic wave theory for transient bed sediment waves in alluvial rivers." *J. Hydrol. Engrg.*, 13(5), 297-304.
88. Smith, H. G. (2008). "Estimation of suspended sediment loads and delivery in an incised upland headwater catchment, south-eastern Australia." *Hydrolog. Process.*, 22(16), 3135-3148.
89. Snyder, F. F. (1938). "Synthetic unit-graphs", *Trans. Am. Geophys. Union*, 19, 447-454.
90. Srinivasulu, S., and Jain, A. (2009). "River flow prediction using an integrated approach." *J. Hydrol. Engrg.*, 14(1), 75-83.
91. Strand, R. I., and Pemberton, E. L. (1987). Reservoir sedimentation in design of small dams, U.S. Bureau of Reclamation, Denver.
92. Sudheer, K. P., Gosain, A. K., and Ramasastri, K. S. (2002). "A data-driven algorithm for constructing artificial neural network rainfall-runoff models." *Hydrolog. Process.*, 16(6), 1325-1330.
93. Sudheer, K. P. Nayak, P. C., and Ramasastri, K. S. (2003). "Improving peak flow estimates in artificial neural network river flow models." *Hydrolog. Process.* 17(3), 677-686.
94. Swamee, P. K. (2001). "Reservoir capacity depletion on account of sedimentation." *Int. J. of Sediment Research*, 16(3), 408-415.

95. The MathWorks, Inc. (2001). *ANN Toolbox User's Guide*, 3 Apple Hill Drive, Natick, MA 01760-2098.
96. Tayfur, G. (2001). "Modelling two-dimensional erosion process over infiltrating surfaces." *J. Hydrol. Engrg.*, 6(3), 259-262.
97. Tayfur, G. (2002). "Applicability of sediment transport capacity models for nonsteady state erosion from steep slopes." *J. Hydrol. Engrg.*, 7(3), 252-259.
98. Tayfur, G., Ozdemir, S., and Singh, V. P. (2003). "Fuzzy logic algorithm for runoff-induced sediment transport from bare soil surfaces." *Adv. Water. Res.*, 26, 1249-1256.
99. Tejuwani, K.G. (1984). "Reservoir sedimentation in India-Its causes, Control, and Future course of action." *Water International*, 9, 150-154.
100. Thirumalaiah, K., and Deo, M.C. (2000). "Hydrological forecasting using neural networks." *J. Hydrol. Engrg.*, 5 (2), 180-189.
101. Tokar, A.S., and Johnson, A. (1999). "Rainfall-runoff modeling using artificial neural networks." *J. Hydrol. Engrg.*, 4(3), 232-239.
102. Tokar, A. S., and Markus, M. (2000). "Precipitation-runoff modelling using artificial neural networks and conceptual models." *J. Hydrol. Engrg.*, 5(2), 156-161.
103. Thomas, W. A., and Prasuhn, A. L. (1977). "Mathematical modelling of Scour and deposition." *J. Hydr. Div.*, 103, HY8, 851-863.
104. Woodward, J.C., and Walling, D. E. (2007). "Composite suspended sediment particles in river systems: their incidence, dynamics and physical characteristics." *Hydrolog. Process.*, 21(26), 3601-3614.

105. Zealand, C. M., Burn, D. H., and Simonovic, S.P. (1999). "Short term streamflow forecasting using artificial neural networks." *J. Hydrol.*, 214(1-4), 32-48.
106. Zhang, B., and Govindaraju, R.S. (2000). "Prediction of watershed runoff using Bayesian concepts and modular neural networks." *Water Resour. Res.*, 36(3), 753-762.